

# Machine learning to inform tunnelling operations: recent advances and future trends

Brian Sheil, Stephen Suryasentana, Michael Mooney and Hehua Zhu

Brian B. Sheil

*Department of Engineering Science, University of Oxford, Parks Road, Oxford OX1 3PJ, UK.*

*Email: [brian.sheil@eng.ox.ac.uk](mailto:brian.sheil@eng.ox.ac.uk)*

*ORCID: 0000-0002-1462-1401*

Stephen K. Suryasentana

*Department of Engineering Science, University of Oxford, Parks Road, Oxford OX1 3PJ, UK.*

*Email: [stephen.suryasentana@eng.ox.ac.uk](mailto:stephen.suryasentana@eng.ox.ac.uk)*

Michael A. Mooney

*Department of Civil and Environmental Engineering, Colorado School of Mines, 1500 Illinois St., Golden, CO 80401, USA.*

*Email: [mooney@mines.edu](mailto:mooney@mines.edu)*

Hehua Zhu

*Department of Geotechnical Engineering, College of Civil Engineering Tongji University, Shanghai 200092, China.*

*Email: [zhuhehua@tongji.edu.cn](mailto:zhuhehua@tongji.edu.cn)*

Initial submission, 27 April 2020

Revised submission, 30 June 2020

2<sup>nd</sup> revised submission, 19 November 2020

Main text wordcount: 5085

Figures: 11

Tables: 3

1   **ABSTRACT**

2   The proliferation of data collected by modern tunnel boring machines (TBMs) presents a  
3   substantial opportunity for the application of machine learning (ML) to support the decision-  
4   making process on site with timely and meaningful information. The observational method is  
5   now well-established in geotechnical engineering and has a proven potential to save time  
6   and money relative to conventional design. ML advances the traditional observational  
7   method by employing data analysis and pattern recognition techniques, predicated on the  
8   assumption of the presence of enough data to describe the modelled system's physics. This  
9   paper presents a comprehensive review of recent advances and applications of ML to inform  
10   tunnelling construction operations with a view to increasing their potential for uptake by  
11   industry practitioners. This review has identified four main applications of machine learning  
12   to inform tunnelling, namely TBM performance prediction, tunnelling-induced settlement  
13   prediction, geological forecasting and cutterhead design optimisation. The paper concludes  
14   by summarising research trends and suggesting directions for future research for ML in the  
15   tunnelling space.

## LIST OF NOTATIONS

1	$\alpha$	Orientation of planes of weakness in rock mass.
2	$\beta_g, \beta_l$	Global and local learning parameters, respectively, for particle swarm optimisation algorithm.
3		
4	$\gamma$	Soil unit weight.
5		
6	$\gamma_{SVM}$	Support vector machine kernel coefficient.
7	$\epsilon$	Gaussian noise.
8	$\zeta(x)$	Gaussian membership function of an input value $x$ .
9	$\theta$	Tunnel boring machine pitching angle.
10		
11	$\kappa$	Slope of soil unload-reload curve.
12	$\mu(x)$	Mean vector of a Gaussian process.
13	$\nu_l$	Poisson's ratio of the tunnel lining.
14	$\nu_s$	Poisson's ratio of the soil.
15		
16	$\rho_1, \rho_2$	Two randomly initiated vectors with entries ranging between 0 and 1.
17	$\sigma$	Standard deviation of the Gaussian function.
18	$\phi'$	Soil friction angle.
19	$\psi'$	Soil dilation angle.
20		
21	$A$	Face area of tunnel boring machine.
22	$a$	Parameter controlling the fuzziness of the system using the fuzzy c-means clustering algorithm.
23		
24	AR	Tunnel boring machine advance rate.
25	$b$	Adjustable bias vector.
26		
27	BI	Brittleness index of rock mass.
28	$C$	Pipe string convergence.
29	$c$	Mean of the Gaussian function.
30	$c'$	Soil cohesion.
31		
32	CP	Cutterhead power.
33	CM	Construction method.
34	$D$	Diameter of tunnel boring machine.
35	$d_j$	Centre of data cluster $j$ .
36		
37	$D_c$	Diameter of tunnel boring machine cutting disc.
38	DPW	Depth between planes of weakness.
39	$E_l$	Young's modulus of tunnel lining.
40	$E_s$	Young's modulus of the soil.
41		
42	EI	Flexural rigidity.
43	EPB	Earth pressure balance.
44	$f(x)$	Latent function representing the underlying structure of the data.
45	FPI	Field penetration index.
46		
47	$g^*$	Global best historical location for particle swarm optimisation algorithm.
48	GSI	Geological strength index.
49	$H$	Tunnel cover depth.
50		
51	$H_w$	Height of groundwater table above tunnel boring machine.
52	$i_t, i_l$	Transverse and longitudinal inflection point of soil surface settlement curve.
53	$J_{FCM}$	Fuzzy c-means clustering objective function.
54	$JF$	Tunnel boring machine jacking force.
55		
56	$K$	Coefficient of lateral earth pressure.
57	$k_s$	Soil permeability.
58	$k_{sub}$	Modulus of subgrade reaction.
59	$k(x, x')$	Covariance function of input pairs $x$ and $x'$ .
60		
61		
62		
63		
64		
65		

1	$L$	Tunnel length.
2	$L_{\epsilon}(y)$	$\epsilon$ -insensitive cost function used in support vector machine algorithm.
3	$M_{ij}$	Fuzzy c-means clustering membership matrix
4	$n_f, n_{hi}, n_o$	The number of features, neurons in hidden layer $i$ and outputs (respectively) in an artificial neural network.
5		
6	$n_p, n_c$	The number of datapoints and clusters respectively using fuzzy c-means clustering.
7		
8	$O$	Open mode hard rock.
9	$P_c$	Chamber pressure.
10	$P_f$	Tunnel boring machine face pressure.
11	$P_g$	Grout pressure.
12	PLS	Point load strength
13	PR	Tunnel boring machine penetration rate.
14	$q$	Rock quartz content.
15	$Q_f$	Conditioning foam flow rate.
16	$R$	Tunnel radius.
17	$R_d$	Soil relative density.
18	RPM	Cutterhead rotational speed.
19	RQD	Rock quality designation
20	RMW	Rock mass weathering
21	RMR	Rock mass rating
22	PSI	Point strength index
23	RMQ	Rock mass quality
24	SBI	Specific rock mass boreability index.
25	$s_c$	Spacing of tunnel boring machine cutting discs.
26	SCP	Screw conveyor power.
27	SER	Specific energy requirement
28	SF	Safety factor against tunnel collapse.
29	$S_{max}$	Maximum soil surface settlement.
30	SPT	Standard penetration test.
31	$s_u$	Undrained shear strength of soil.
32	$S(X, Y)$	Soil surface settlements at settlement monitoring point position at $X, Y$ .
33	$t$	Time.
34	$T$	Cutterhead torque.
35	$t_c$	Thickness of tunnel boring machine cutting disc.
36	$t_l$	Tunnel lining thickness
37	UCS	Unconfined compressive strength of rock mass.
38	$U_{max}$	Maximum horizontal soil displacement.
39	$V_g$	Volume of grout.
40	$v_i$	Velocity of particle $i$ used in particle swarm optimisation algorithm.
41	$V_L$	Volume loss.
42	$w$	Adjustable weights vector.
43	$w_c$	Soil water content.
44	WT	Elevation of groundwater table.
45	$X$	Horizontal (transverse) distance to settlement monitoring point.
46	$x_i^*$	Local (for particle $i$ ) best historical location for particle swarm optimisation algorithm.
47	$Y$	Horizontal (longitudinal) distance to settlement monitoring point ahead of the face of the tunnel boring machine.
48		
49		
50		
51		
52		
53		
54		
55		
56		
57		
58		
59		
60		
61		
62		
63		
64		
65		

## 16 INTRODUCTION

1  
2  
3 17 Rapid urbanisation points to the use of underground space as one of the most viable,  
4  
5 18 sustainable and efficient means of delivering new services and transport in congested urban  
6  
7 19 areas. The use of trenchless technology in infrastructure construction is growing in popularity  
8  
9  
10 20 for its cost and environmental savings compared to conventional open excavation  
11  
12 21 techniques (Royston et al. 2020). In these obstructed underground spaces, optimising the  
13  
14 22 performance of tunnelling operations is critical to ensure safe and economical construction  
15  
16 23 while also preventing damage to existing infrastructure both above and below ground (Chieh  
17  
18  
19 24 et al. 2020).

20  
21  
22 25 Traditionally, tunnelling contractors have relied on empiricism, in addition to more formal  
23  
24 26 design calculations. While simplified design calculations play an important role in tunnel  
25  
26 27 design and construction, optimising tunnelling operations remains technically challenging  
27  
28 28 due to their dependence on several complex factors such as site geology, tunnel boring  
29  
30  
31 29 machine (TBM) operational parameters and tunnel geometry (O'Dwyer et al. 2018, 2019,  
32  
33 30 Phillips et al. 2019). Although a significant body of research conducted over the last thirty  
34  
35 31 years has greatly enhanced our understanding of these effects and their influence on  
36  
37 32 tunnelling operations, the literature contains many examples where static 'rule-based' design  
38  
39 33 methods fail to provide satisfactory prediction of field behaviour e.g. Barla et al. (2006), Choo  
40  
41  
42 34 and Ong (2015), Sheil et al. (2016).

43  
44  
45 35 The proliferation of data collected by modern TBMs presents a substantial opportunity for the  
46  
47 36 application of machine learning (ML) to support the decision-making process on site with  
48  
49 37 timely and meaningful information (Sheil et al. 2020). While Shreyas and Dey (2019) present  
50  
51 38 a high level overview of machine techniques for tunnelling settlement and performance  
52  
53 39 prediction, a more comprehensive review of recent advances and applications of ML to  
54  
55 40 inform tunnelling construction operations is necessary to increase their potential for uptake  
56  
57 41 by industry practitioners. To this end, this review has identified four main applications of  
58  
59  
60  
61  
62  
63  
64  
65

1  
2  
3  
4  
5  
6  
7  
8  
9  
10  
11  
12  
13  
14  
15  
16  
17  
18  
19  
20  
21  
22  
23  
24  
25  
26  
27  
28  
29  
30  
31  
32  
33  
34  
35  
36  
37  
38  
39  
40  
41  
42 machine learning to inform tunnelling, namely TBM performance prediction, tunnelling-  
43 induced settlement prediction, geological forecasting and cutterhead design optimisation.  
44 The paper concludes by summarising research trends and suggesting directions for future  
45 research for ML in the tunnelling space.

## 46 47 **MACHINE LEARNING MODELS**

### 48 *Overview*

49 The practice of ML has experienced immense recent growth, driven by advances in  
50 computational performance, sensing technology and data storage. In geotechnical  
51 engineering, ML advances the traditional observational method by employing data analysis  
52 and pattern recognition techniques, predicated on the assumption of the presence of enough  
53 data to describe the modelled system's physics. These observational techniques have a  
54 proven potential to save time and money relative to conventional design (e.g. Sheil et al.  
55 2018, Royston et al. 2020).

56 Artificial intelligence (AI), ML and deep learning are three terms often used interchangeably  
57 to describe software that behaves in an intelligent manner. ML is a subset of AI which  
58 provides systems with the ability to automatically learn and perform certain tasks without  
59 being explicitly programmed. The most common implementation of ML involves the  
60 development of relationships between inputs and outputs. In the case where outputs are  
61 provided known labels (i.e. the correct outputs are known) then the learning process is  
62 referred to as 'supervised'. This contrasts with 'unsupervised' learning where instances do  
63 not have corresponding labels. Deep learning is a further subset of ML which uses a specific  
64 ML algorithm called 'deep' artificial neural networks, with many hidden layers, to learn from  
65 large amounts of data.

66 A drawback of many supervised learning techniques is the requirement for a large database  
67 of high-quality information to accurately capture the physics of the modelled system. The  
68 size of the dataset required for the training process is highly dependent on the type of ML  
69 technique adopted, its intended role (e.g. interpolation, optimisation, forecasting) and the  
70 complexity of the input-output relationship being modelled. This section provides a brief  
71 overview of ML techniques commonly applied to tunnelling operations.

72

### 73 *Artificial neural networks*

74 An artificial neural network (ANN) is an information processing paradigm that draws inspiration  
75 from the operation of the human brain. A network consists of multiple interconnected layers of  
76 neurons, comprising a layer of input neurons, one or more layers of 'hidden' neurons that  
77 perform operations on the data, and a layer of output neurons. Transformation of the input  
78 data is performed by the artificial neurons through the application of a nonlinear function  
79 (known as the activation function) of the sum of weighted inputs (see Fig. 1). In its simplest  
80 form (a feedforward neural network), data travels in one direction – from input to output. After  
81 each complete iteration, termed 'epochs', the network output values are compared to the  
82 target values to produce an error measurement. Feedback of the error through the network,  
83 known as 'backpropagation', is a nonlinear optimisation process which adjusts the weight and  
84 bias of each connection towards reducing the value of the cost function. In this paper the  
85 'architecture' describes the network structure in the form  $n_f \dots n_{hi} \dots n_o$  where  $n_f$ ,  $n_{hi}$  and  $n_o$  are  
86 the number of features, neurons in hidden layer  $i$  and outputs respectively.

87 An alternative network form is a recurrent neural network (RNN) wherein connections between  
88 units form a directed cycle. This allows the network to maintain information in 'memory' over  
89 time and therefore use historical calculations to determine outputs. Long short-term memory  
90 (LSTM) is a type of RNN that uses a 'memory cell' that can store information for long periods  
91 of time. A set of 'gates' are used to decide whether information is stored in the memory cell,

92 when information from the memory cell is deployed in the network or when information is  
93 removed from the cell altogether (i.e. forgotten).

94

### 95 *Fuzzy logic*

96 Fuzzy logic (FL) involves the integration of expert knowledge and experience into a fuzzy  
97 inference system using fuzzy 'If-Then' rules to model the qualitative aspects of human  
98 knowledge. This allows an extension of binary, classic logic to qualitative, subjective and  
99 approximate situations. Takagi and Sugeno (1985) presented the first systematic  
100 investigation of fuzzy modelling. The purpose of a fuzzy inference system is to map inputs to  
101 outputs through the application of fuzzy reasoning. Fuzziness is first applied to the inputs to  
102 produce a fuzzy set using a 'membership function',  $\zeta(x)$ , such as the Gaussian membership  
103 function:

$$\zeta = e^{-\frac{(x-c)^2}{2\sigma^2}} \quad (1)$$

104 where  $x$  is the input value and  $\sigma$  and  $c$  are the standard deviation and mean of the Gaussian  
105 function, respectively. The resulting fuzzy set is processed using a set of If-Then rules. The  
106 results are subsequently defuzzified to produce 'crisp' outputs.

### 108 *Adaptive neuro-fuzzy inference systems*

109 Adaptive neuro-fuzzy inference systems (ANFIS) denotes the fusion of neural networks with  
110 fuzzy logic principles. The key difference to traditional neural networks is that part or all  
111 nodes in the network are modified to be 'adaptive'. This means that the outputs of the  
112 network are now dependent on the nodal parameters and the learning rule updates the  
113 parameters to minimise a prescribed error measurement. Relationships between variables  
114 are defined using fuzzy If-Then rules. ANFIS networks are typically organised in five layers  
115 as follows: (a) layer 1 is the input layer comprising the adaptive nodes and node functions

116 and activates the fuzziness of the inputs, (b) layer 2 determines the firing strength of each  
117 rule, (c) layer 3 normalises the firing strengths, (d) layer 4 defines the consequence  
118 parameters and (e) layer 5 computes the ANFIS outputs by summing the outputs of layer 4.

119

### 120 *Fuzzy c-means clustering*

121 Conventional clustering techniques assign data to a cluster without consideration of the  
122 extent of its 'belonging' to that cluster. First introduced by Dunn (1974), fuzzy c-means  
123 clustering (FCM) is a clustering approach that allows a datapoint to belong to multiple  
124 clusters with varying degrees of membership. This method uses an iterative clustering  
125 technique to produce an optimal 'd' through the minimisation of an objective function  $J_{FCM}$ :

$$J_{FCM} = \sum_{i=1}^{n_p} \sum_{j=1}^{n_c} M_{ij}^a \|x_i - d_j\|^2 \quad (2)$$

126 where  $n_p$  and  $n_c$  are the number of datapoints and clusters respectively,  $M_{ij}$  is the  
127 membership matrix,  $a > 1$  is a parameter controlling the fuzziness of the system and  
128  $\|x_i - d_j\|^2$  is the squared Euclidian distance between observation  $x_i$  and cluster centre  $d_j$ .

129

### 130 *Classification and regression trees and random forest*

131 Classification and regression trees (CART) are a non-parametric method that build  
132 classification or regression models in the form of a tree structure. At each tree node, a  
133 specified number of features are randomly selected and tested to achieve an optimal split of  
134 the data. Although decision trees can be highly effective, they are prone to overfitting and are  
135 sensitive to the specific dataset upon which they are trained. A robust solution to overfitting is  
136 the concept of random forests, first proposed by Breiman (2001). Random forest (RF) is an  
137 ensemble learning method that operates by building multiple decision trees and aggregating  
138 the results (see Fig. 2). Multiple different training sets (termed bootstrap samples) are

139 generated by sampling with replacement randomly from the original data. This method builds  
140 several instances of a decision tree which produces an output  $\hat{y}_i$  corresponding to each tree.  
141 All individual outputs are then averaged to obtain the final prediction,  $\hat{y}$ .

142

### 143 *Gaussian process regression*

144 A Gaussian process is a collection of random variables of which any finite number follow a  
145 joint Gaussian distribution (Williams and Rasmussen, 1996). Gaussian process regression  
146 (GPR) provides a method to perform Bayesian inference about functions in a non-parametric  
147 way. One of the key aspects of GPRs is the use of covariance functions which encodes prior  
148 assumptions about the functions one wishes to learn (in this case the measured data). This  
149 avoids reliance on algebraic mapping between inputs and outputs. The overall aim of the  
150 process is to learn a regression model of the form  $y = f(x) + \epsilon$ , where  $f(x)$  is a latent function  
151 representing the underlying structure of the data and  $\epsilon \sim N(0, \sigma^2)$  is a Gaussian noise term  
152 where  $\sigma^2$  is the variance of the noise (the symbol ' $\sim$ ' means 'distributed according to'). A GP  
153 can be completely described by a mean vector,  $\mu(x)$ , and covariance function  $k(x, x')$  of input  
154 pairs  $x$  and  $x'$  to describe an underlying real process  $f(x)$  as follows:

$$f(x) \sim \mathcal{GP}(\mu(x), k(x, x')) \quad (3)$$

155 where

$$\mu(x) = \mathbb{E}[f(x)] \quad (4)$$

$$k(x, x') = \mathbb{E} \left[ (f(x) - \mu(x))(f(x') - \mu(x'))^T \right] \quad (5)$$

156

### 157 *Support Vector Machine/Regression*

158 The term 'support vector regression' (SVR) denotes the application of support vector machines  
159 (SVM) to regression problems. The  $\epsilon$ -insensitive approach first proposed by Vapnik (1995) is  
160 one of the most widely adopted SVM/SVR approaches in the literature. SVR uses either linear

161 or non-linear kernels to map the input space into a high-dimensional feature space. The most  
 162 common kernel adopted for this purpose is the radial basis function (RBF):

$$k(x_i, x) = \exp(-\gamma_{\text{SVM}} \|x_i - x\|^2) \quad (6)$$

163 where  $\gamma_{\text{SVM}}$  is a kernel coefficient. A hyperplane is subsequently constructed in the feature  
 164 space where the quality of fit to the data is computed using an  $\epsilon$ -insensitive cost function  
 165 ( $L_\epsilon(y)$ ) defined as follows (see Fig. 3):

$$L_\epsilon(y) = \begin{cases} 0 & \text{for } |f(x) - y| \leq \epsilon \\ |f(x) - y| - \epsilon & \text{otherwise} \end{cases} \quad (7)$$

166 where  $x$  is the input data with target values  $y$ ,  $f(x)$  is the regression function, and  $\epsilon$  is a  
 167 user-defined positive value representing the maximum distance between  $f(x)$  and  $y$  for which  
 168 there is no loss in the cost function. According to equation (7), only predictions that have  
 169 residuals greater than  $\epsilon$  are penalised, while predictions with smaller residuals have no effect  
 170 on the regression equation. Considering a linear function as an example,  $f(x)$  can be defined  
 171 as follows:

$$f(x) = (\mathbf{w} \cdot x) + b \quad (8)$$

172 where  $\mathbf{w}$  is an adjustable weight vector and  $b$  is the bias. The objective is to obtain a function  
 173 that has the smallest  $\epsilon$  deviation from the target values in the training data and is also as 'flat'  
 174 as possible (by minimising the Euclidean norm  $\|\mathbf{w}\|^2$ ).

### 176 *Extreme learning machine*

177 Extreme learning machine (ELM) is a three-layer neural network i.e. it comprises a single  
 178 hidden layer (Huang et al. 2004). The novelty of ELM centres around its use of randomly  
 179 generated hyperparameters for the hidden layer which are not updated during training,  
 180 unlike conventional neural networks (Huang et al. 2006). This significantly reduces the  
 181 computational time associated with the learning process and increases the network's ability

182 to generalise within the trained parameter space. The ELM training process involves the  
 183 generation and selection of random numbers for the weight and bias matrices for the hidden  
 184 layer (Huang et al. 2011). Since the number of neurons in the hidden layer is typically much  
 185 less than the number of training observations, the network is an over-determined linear  
 186 system. A consequence of this is that the output weight matrix is the only parameter that  
 187 needs to be optimised during training, which can be undertaken using an ordinary least  
 188 squares approach.

189

### 190 *Particle swarm optimisation*

191 Particle swarm optimisation (PSO) is an optimisation algorithm developed by Kennedy and  
 192 Eberhart (1995). This approach attempts to mimic interactions in groups of social beings and  
 193 the sharing of information between the group members (termed ‘particles’). Rather than  
 194 using a single particle to search for an optimal solution, the whole population is used where  
 195 the velocities of each member are defined by both a stochastic and deterministic component.  
 196 While each particle moves randomly, it is partially guided by its own (local) best position as  
 197 well as the best position of the group (global). The updated velocity vector at time  $t+1$  for  
 198 particle  $i$  ( $v_i^{t+1}$ ) is defined as follows:

$$v_i^{t+1} = v_i^t + \beta_g \rho_1 (g^* - x_i^t) + \beta_l \rho_2 (x_i^* - x_i^t) \quad (9)$$

199 where  $\rho_1$  and  $\rho_2$  are two randomly initiated vectors with entries ranging between 0 and 1,  $\alpha$   
 200 and  $\beta$  are the global and local learning parameters respectively,  $x_i$  is the position of particle  $i$   
 201 and  $g^*$  and  $x_i^*$  are the global and local (for particle  $i$ ) best historical location.

202

### 203 *Evolutionary algorithms*

204 First proposed by Holland (1992), genetic algorithms (GA) are arguably the most popular  
205 variant of the evolutionary algorithm. These methods are a computational model inspired by  
206 evolution and the mechanisms of natural selection and are typically deployed as search and  
207 optimisation algorithms. The parameters of the user-defined search space are first encoded  
208 in the form of chromosomes which can in turn be grouped to form a population. The process  
209 begins by initiating a random population representing different nodes in the search space.  
210 The fitness (cost) function is then evaluated for each node to determine the fitness value.  
211 New search nodes are randomly generated by applying genetic operations on the nodes  
212 based on their fitness values. This process is repeated until an optimal solution is acquired.  
213 The purpose of the genetic operators is to combine the 'good' structures of each node to  
214 produce an improved search node. Common genetic operators are shown in Fig. 4 and  
215 include (a) crossover (portions of chromosomes are swapped), (b) reproduction  
216 (chromosomes with good fitness values in an old population are preserved in the new  
217 population) and (c) mutation (occasional random alteration of a chromosome).

218 Three alternative evolutionary algorithms include (a) genetic programming (GP), (b) gene  
219 expression programming (GEP) and (c) differential evolution (DE). The fundamental  
220 difference between these approaches lies primarily in the composition of the individuals  
221 within the respective populations. In GAs, individuals are linear chromosome strings of fixed  
222 length; in GPs, they are non-linear units with varying shapes and sizes; in GEPs, they are  
223 encoded linear strings of fixed length (similar to GA chromosomes) which are subsequently  
224 expressed as non-linear units of varying shapes and sizes; and in DEs, they are real vectors  
225 rather than binary chromosome strings.

### 227 *Imperialist competitive algorithm*

228 The imperialist competitive algorithm (ICA) is an alternative evolutionary search and  
229 optimisation algorithm proposed by Atashpaz-Gargari and Lucas (2007) and is derived from

230 human being's socio-political evolution. In this case, the initial population is termed  
231 'countries' and is broken into two categories: (a) colony and (b) imperialist. A cost function is  
232 used to determine which countries of the initial population are the most 'powerful' and are  
233 therefore selected as imperialist states. The remaining countries are assigned as colonies of  
234 the imperialist states depending on the value of the cost function for each imperialist state.  
235 The imperialist state and their respective colonies are denoted an empire. The ensuing  
236 optimisation process is described by Fig. 5.

237

## 238 **MACHINE LEARNING IN TUNNELLING**

### 239 *Overview*

240 A wide range of ML techniques have been developed for tunnelling applications. Research  
241 areas have included TBM automation (Mokhtari and Mooney 2019), tunnel condition  
242 assessment (Li et al. 2017, Chen et al. 2019c, Zhu et al. 2020), anomaly detection (e.g. Yu  
243 et al. 2018, Sheil et al. 2020), tunnel profile measurement (e.g. Xue and Zhang 2019),  
244 resilience assessment (e.g. Khetwal et al. 2019), structural defect identification (e.g. Ding et  
245 al. 2019), tunnel face stability (e.g. Hayashi et al. 2019), rockburst prediction (e.g. Liu and  
246 Hou 2019) and intelligent building information modelling (e.g. Zhao et al. 2019b). This review  
247 focuses on four tunnelling applications where the use of ML has been most prevalent: (a)  
248 TBM performance prediction, (b) tunnel-induced settlement prediction, (c) geological  
249 forecasting and (d) cutterhead design optimisation.

250

### 251 *TBM performance prediction*

252 A large body of research has focused on the development of improved TBM performance  
253 predictions by leveraging recent advances in ML. Table 1 presents an overview of these

254 studies where the corresponding parameters and notation are defined in Fig. 6 (a slurry  
1 pressure balance shield machine is shown for illustrative purposes) and Table 2. Research  
2 255 into TBM performance has largely been confined to open mode TBM tunnelling in rock with  
3  
4 256 only a handful of efforts with slurry or earth pressure balance shield TBMs in softer soils  
5  
6 257 (e.g., Mooney et al. 2018, Mokhtari et al. 2020, Mokhtari and Mooney 2020). Mooney et al.  
7  
8 258 (2018) note that maintenance of earth pressure balance (EPB), TBM guidance using thrust  
9  
10 259 and articulation jacks, scraping and imbibing of the in-situ ground and muck processing  
11  
12 260 through a de-pressurizing screw conveyor combine to make performance prediction of EPB  
13  
14 261 TBMs particularly challenging.  
15  
16  
17  
18  
19  
20

21 263 From Table 1, it is notable that penetration rate (PR) is the most favoured measure of TBM  
22  
23 264 performance, defined as the penetration along the axis of the tunnel per unit tunnelling time  
24  
25 265 (i.e. down times/stoppages are not included in the calculation). It can be observed that the  
26  
27 266 input parameters are dominated by ground (rock) properties, with UCS being the most  
28  
29 267 common. For example, Bernardos and Kaliampakos (2004) represent one of the earliest  
30  
31 268 studies to use rock mass properties (e.g. UCS, RMR, weathering) as inputs to an ANN for  
32  
33 269 TBM performance prediction where an error of 6-8% was obtained. For softer soils, Mooney  
34  
35 270 et al. (2018) noted that the TBM performance was most influenced by cutterhead torque,  
36  
37 271 foam flow rate, and screw conveyor rotation speed. It is noteworthy that the selection of input  
38  
39 272 parameters has predominantly been guided by empiricism from previous literature and the  
40  
41 273 application of more robust 'feature engineering' techniques in this area has been limited.  
42  
43 274 Using principal component analysis, Salimi et al. (2015, 2016, 2019) confirmed the strong  
44  
45 275 dependence of TBM performance on rock mass parameters (e.g. UCS, RQD, joint spacing  
46  
47 276 and condition) for hard rock tunnelling.  
48  
49  
50  
51  
52

53 277 Another interesting observation is the inusitation of TBM operational (e.g. jacking force (JF),  
54  
55 278 cutterhead torque (T), cutterhead rotation speed (RPM), slurry parameters, etc) and  
56  
57 279 geometric parameters (e.g. tunnel diameter, distance from reception shaft, soil cover etc) as  
58  
59 280 features. This is because many of the training datasets relate to a single construction project  
60  
61  
62  
63  
64  
65

1  
2 282 and it is a common assumption that TBM and geometric parameters remain constant during  
3 a given project and so should not be included in the ML. While this provides good  
4 283 predictability on a case-by-case basis (where one might wish to forecast the performance of  
5 the TBM for the current project based on the data gathered thus far), it limits the applicability  
6 284 of these trained ML models to other projects. This is particularly important in the case of ML  
7 models as they typically demonstrate a poor ability to extrapolate beyond their calibration  
8 285 space (Ahmed et al. 2010). Recent studies incorporating the influence of TBM operational  
9 parameters for performance prediction have demonstrated an improved ability to generalise  
10 e.g. to alternative excavation techniques (Song et al. 2019).

11 290 The most common ML technique adopted for the prediction of TBM performance is a multi-  
12 layer feedforward ANN with back propagation. The main difference between the ANN  
13 291 models adopted in the literature is the optimal ANN architecture that was ultimately selected.  
14 Even though similar input parameters and datasets have been employed across various  
15 292 studies, the range of architectures that have been adopted is quite wide. For example,  
16 Armaghani et al. (2017) and Koopialipour et al. (2019c) adopted a 7-11-1 ( $n_f-n_{h1}-n_o$ ) and 5-8-  
17 293 32-8-1 architecture respectively for the prediction of the same dataset (the Pahang-Selangor  
18 raw water transfer tunnel (PSWRT)). It is noteworthy that the use of several hidden layers  
19 and neurons increases the likelihood of encountering overfitting. Hecht-Nielsen (1987)  
20 proved that any continuous function can be represented by a neural network using a single  
21 294 layer with  $n_{h1} = 2n_f + 1$  nodes, albeit using significantly more complex activation functions  
22 than the conventional sigmoidal functions commonly adopted in the literature. This  
23 295 corresponds to an architecture of 7-15-1 and 5-11-1 respectively for these studies.

24 303 Other popular ML methods adopted in the literature include fuzzy logic, due to its ability to  
25 incorporate empirical evidence/experience and, recently, more flexible and non-linear ML  
26 304 algorithms such as CARTs (e.g. Xu et al. 2019) and RFs (e.g. Tao et al. 2015). To develop  
27 improved methods for the determination of the optimum architecture and the avoidance of  
28 305 local minima, hybrid methods have also been explored by fusing ML models with

1  
2 308 optimisation algorithms such as ICA (e.g. Naghadehi et al. 2019), PSO (e.g. Armaghani et  
3 al. 2018), DE (e.g. Fattahi and Babanouri 2017) and FCM (e.g. Fattahi 2016).

4  
5 310

6  
7  
8 311 *Tunnelling-induced settlement prediction*

9  
10  
11 312 Table 3 presents an overview of ML models adopted for the prediction of tunnelling-induced

12  
13 313 soil settlements,  $s$ , as well as tunnel convergence,  $C$ . Given the complex nature of

14  
15 314 tunnelling-induced settlements, the number of features used in these models are notably

16  
17 315 greater. Furthermore, these features comprise a mix of soil, tunnel geometry and TBM

18  
19 316 operational parameters. For the studies considered in this review, ANNs appear to have

20  
21 317 been the ML model of choice pre-2012, although they continue to appear in more recent

22  
23 318 literature. It is again apparent that a wide range of architectures have been explored from the

24  
25 319 47-47-47-47-2 architecture adopted by Kim et al. (2001) to the more compact 3-4-1

26  
27 320 architecture proposed by Hasanipanah et al. (2016) and Moghaddasi and Noorian-Bidgoli

28  
29 321 (2018).

30  
31  
32 322 While the integration of fuzzy systems has also been used to predict tunnel-induced

33  
34  
35 323 settlements, the use of SVMs became popular post-2012, quickly followed by more complex

36  
37 324 and non-parametric methods such as CARTs and RFs. The prominence of these methods

38  
39 325 for settlement prediction is perhaps explained by the increased complexity of the input-

40  
41 326 output mapping process for tunnelling-induced settlements. The datasets used for predicting

42  
43 327 tunnel-induced settlements are also largely based on a single project rather than multiple

44  
45 328 projects, with the size of the dataset varying considerably (from 6 to 7650 datapoints).

46  
47  
48  
49  
50  
51  
52 329

53  
54  
55 330 *Geological forecasting*

331 Efforts to predict ahead of the TBM involve identification of geological conditions as well as  
1  
2 332 the size and location of potential obstacles (Schaeffer & Mooney 2016). In these cases, it is  
3  
4 333 desirable to identify changes in soil conditions as shown in Fig. 7. To obtain actionable  
5  
6 334 information during tunnelling, soil conditions must be forecasted sufficiently far in advance of  
7  
8 335 the TBM (typically metres to tens of metres). This is complicated by a deterioration in the  
9  
10 336 accuracy of forecasting techniques with an increase in the forecast horizon.

11  
12  
13  
14 337 One approach is to consider the TBM itself as an exploratory tool. A popular implementation  
15  
16 338 of this approach is to first use statistical interpolation techniques (such as kriging) to develop  
17  
18 339 an initial estimate of the ground conditions at the TBM face using available borehole  
19  
20 340 information as shown in Fig. 8 (Gangrade and Mooney 2019, Grasmick et al. 2020). These  
21  
22 341 predictions are subsequently updated using TBM driving data to obtain a more reliable  
23  
24 342 estimate of the ground immediately ahead of the TBM. This methodology has been adopted  
25  
26 343 by Yamamoto et al. (2003) and Sun et al. (2018b). In particular, Sun et al. (2018b) achieved  
27  
28 344 a prediction accuracy of  $R^2 = 0.8$  using RFs.

29  
30  
31  
32  
33 345 Alternatively, ML can also be used to provide a direct mapping between TBM performance  
34  
35 346 parameters and ground conditions. This approach can be considered the inverse of the  
36  
37 347 techniques reviewed for TBM performance prediction. Liu et al. (2019) used SVR combined  
38  
39 348 with a stacked single-target technique to identify multiple targets from a common dataset,  
40  
41 349 such as UCS, BI, DPW and  $\alpha$ ; this allowed correlation between targets to be incorporated  
42  
43 350 into the prediction model. The driving data used to identify the target variables included  
44  
45 351 RPM, PR, JF, T and cutterhead power (CP) where a prediction accuracy of  $R^2$  between 0.63  
46  
47 352 and 0.83 was achieved. It is notable that  $R^2 = 0.83$  corresponded to the UCS prediction  
48  
49 353 indicating its strong correlation with TBM performance in rock. Zhang et al. (2019c) used  
50  
51 354 SVM, RF and  $k$ -nearest neighbours (kNNs) to map RPM, T, JF and AR to rock mass type.  
52  
53 355 Zhao et al. (2019a) compared the performance of eight ML models to predict geological type  
54  
55 356 using feature augmentation to improve performance; a traditional ANN was found to provide  
56  
57 357 the best performance. Jung et al. (2019) also used an ANN to predict the ground type from  
58  
59  
60  
61  
62  
63  
64  
65

1  
2 359 PR, JF and T with an accuracy of  $R^2 > 0.9$ . The PR parameter was found to be the most  
3  
4 360 influential for predicting ground type, particularly across different sites. Liu et al. (2020) used  
5  
6 361 a hybrid algorithm combining traditional ANNs with simulated annealing to predict rock  
7  
8 362 parameters UCS, BI, DPW and  $\alpha$  from RPM, T, JF, PR ( $R^2$  between 0.66 and 0.85). Erharter  
9  
10 363 et al. (2019, 2020) used ensemble LSTM networks to classify TBM data into rock behaviour  
11  
12 364 types according to four geological 'indicators'. Yu and Mooney (2020) employed multinomial  
13  
14 365 logistic regression to characterize the fractional representation of four encountered soil types  
15  
16 366 (sand, clay, silt, till deposits) by an EPB TBM. The regression model was trained using RPM,  
17  
18 367 AR, chamber pressure, excavated soil mass, thrust force, and 83 boring logs along the  
19  
20 alignment.

21  
22  
23 368 Instead of using TBM operational parameters, Zhuang et al. (2018) used convergence  
24  
25 369 displacements in rock to infer  $E_s$  and  $v_s$  through inverse analysis. This involved the use of  
26  
27 370 SVR which is optimised using multi-strategy artificial fish swarm algorithm (MAFSA). The  
28  
29 371 MAFSA approach is an ensemble algorithm comprising differential evolution, particle swarm  
30  
31 372 optimization, adaptive step size and phased vision strategy based on artificial fish swarm  
32  
33 373 algorithm (AFSA) to enhance the global search capability and improve convergence speed  
34  
35 374 and optimization accuracy.

36  
37  
38  
39  
40 375 While numerous geophysical methods have been explored for forecasting geological  
41  
42 376 conditions ahead of the TBM face (e.g. electromagnetic methods, electrical methods,  
43  
44 377 seismic reflection methods, infrared detection methods), very few studies have explored the  
45  
46 378 integration of machine learning algorithms to improve geophysical predictions. Both  
47  
48 379 Alimoradi et al. (2008) and Von and Ismail (2017) used an ANN to identify rock  
49  
50 380 characteristics using ground parameters obtained from Tunnel Seismic Prediction (TSP)  
51  
52 381 technology. Although Von and Ismail (2017) reported a prediction accuracy of  $R^2 = 0.85$ ,  
53  
54 382 they noted that the small datasets at the beginning of a project lead to less reliable  
55  
56 383 predictions.

384 Wei et al. (2018) documented one of the most comprehensive applications of ML to a new  
1  
2 385 'Tunnel Look-ahead Imaging Prediction System' (TULIPS). The TULIPS imaging approach  
3  
4 386 comprises three sets of GPR antennae (low frequency for long-range inspection and two  
5  
6 387 high frequencies to identify small objects) and seismic imaging. The pipeline of their event  
7  
8 388 detection and tracking method is outlined in Fig. 9. An experimental campaign showed that  
9  
10  
11 389 buried obstacles can be successfully identified and tracked using this methodology. Those  
12  
13 390 authors also recommended the development and application of more robust ML models to  
14  
15 391 larger datasets including expert interpretations and ground prediction, and TBM and  
16  
17 392 geological exploration data.  
18  
19  
20  
21 393

#### 24 394 *Cutterhead design optimisation*

27 395 The final research area covered by this literature review is the optimisation of the cutterhead  
28  
29 396 design (see Fig. 10) which appear to have focused exclusively on tunnelling in rock.

32 397 Literature in this area can be further categorised as an optimisation of (a) cutter disc layout  
33  
34 398 and (b) cutter disc geometry. For the cutter layout, the optimisation process has been  
35  
36 399 typically undertaken to (a) minimise eccentric forces (and therefore moments) of the whole  
37  
38 400 system by maximising cutterhead symmetry, (b) maximise excavation efficiency by ensuring  
39  
40 401 adjacent cutters score the tunnel face successively and (c) minimise excavation-induced  
41  
42 402 stress on the cutterhead (e.g. Ji et al. 2016). Other common constraints include (a) cutter  
43  
44 403 discs must remain contained within the cutterhead, (b) cutter discs must not overlap, (c)  
45  
46 404 cutter discs must not interfere with manholes, 'buckets' or joints in the cutterhead, and (e)  
47  
48 405 cutter disc positions should be easily accessible for maintenance (Rostami and Chang  
49  
50 406 2017).  
51  
52  
53  
54

55 407 An example optimisation documented by Huo et al. (2010, 2011) using a multi-objective GA  
56  
57 408 and co-evolutionary GA is presented in Fig. 11. Those authors used three 'base' designs as  
58  
59 409 the starting point for the optimisation to reflect current designs used in practice: a multi-spiral  
60  
61  
62  
63  
64  
65

410 (Fig. 11(a)), 'dynamic star' (Fig. 11(b)) and stochastic pattern (Fig. 11(c)). Another possible  
411 reason for the use of these base designs is that the results of the optimisation process were  
412 reported to be highly dependent on the initial cutter pattern. This was also discovered by Qi  
413 et al. (2013) using grey rational analysis. Grey rational analysis (GRA) is a form of grey  
414 system theory (proposed by Deng (1982)) and solves multiple attribute decision making by  
415 combining the entire range of attribute values being considered for each alternative decision  
416 into a single value (Kuo et al. 2008). Those authors also found that the polar angle played a  
417 more important role on the cutter layout rather than radial distance from the centre point of  
418 the cutterhead. Although not discussed in those studies, these findings suggest the  
419 occurrence of local optima in these optimisation problems. While multiple alternative  
420 optimisation algorithms exist (e.g. grid search, random search), Bayesian optimisation  
421 (Brochu et al. 2010) seems suitable for this problem given its robustness to local optima.  
422 This is due to its exploration versus exploitation strategy: exploitation initially steers the  
423 search process into the direction of the local optima but exploration allows the algorithm to  
424 'escape' from the local optimum towards finding an improved global optimum.

425 On the geometric design of individual cutters, Xia et al. (2012) and Xia et al. (2015) used GA  
426 and multi-objective and multi-geologic conditions optimisation (MMCO) to optimise the (a)  
427 cutter cutting edge angle, (b) cutting edge width, (c) transition arc radius and (d) caulking  
428 ring width between bearings. The optimisation process sought to minimise the cutter bearing  
429 load.

430

## 431 **SUMMARY**

432 This review has identified an increasing trend in the use of ML in the tunnelling space with a  
433 significant increase in 2019. It is likely that this trend will persist as advancements in ML  
434 continue to be translated into practical domains for routine use and more tunnelling data is  
435 shared with the academic community. ANNs have experienced sustained popularity in this

1  
2 437 area. This is not surprising as ANNs are one of the oldest ML paradigms and are able to  
3 capture complex non-linear relationships and generalise within the trained parameter space.  
4 438 The second most popular technique is SVR/SVM. The non-parametric nature of these  
5 models means that model complexity remains relatively unaffected by an increase in the  
6 439 number of features and are therefore particularly suited to high-dimensional datasets. This  
7 may go some way to explaining their popularity, particularly for settlement predictions due to  
8 440 the larger number of influencing factors. These techniques have been typically coupled with  
9 optimisation algorithms to overcome the slow tuning process of the kernel hyperparameters.  
10  
11 441 The use of fuzzy-based methods such as ANFIS and FL in this area stems from their ability  
12 to incorporate human experience and their ability to deal with imprecise and noisy data  
13 442 typical of construction monitoring projects. These methods have not experienced the same  
14 growth, which is probably due to the increase in 'big data' in tunnelling that lends itself to  
15 443 training more robust algorithms. It is also apparent that there has been a significant and  
16 recent increase in the use of alternative ML algorithms such as GEP and RF. These models  
17 provide a higher level of performance for the sake of model interpretability and can therefore  
18 444 capture highly non-linear trends. The use of probabilistic ML techniques, such as Bayesian  
19 networks and Gaussian process regression, for underground construction applications have  
20 become more popular in recent years e.g. Zhang et al. (2016), Wang et al. (2017), Chen et  
21 445 al. (2019d), Zhu (2019). These methods are well-conditioned for dealing with noisy and  
22 incomplete data typical of a construction site and perform predictions within a principled  
23 446 framework; in light of this, they represent the most promising techniques for future  
24 applications of ML to inform tunnelling operations.  
25  
26  
27  
28  
29  
30  
31  
32  
33  
34  
35  
36  
37  
38  
39  
40  
41  
42  
43  
44  
45  
46  
47  
48  
49  
50  
51  
52  
53

## 54 459 **CONCLUSIONS AND FUTURE PERSPECTIVES**

57 460 This paper has presented a comprehensive review of the literature exploring the use of  
58 machine learning to inform tunnelling operations. While machine learning has been used to  
59  
60  
61  
62  
63  
64  
65

1  
2 462 inform a wide range of tunnelling applications, this review has identified four main areas of  
3  
4 463 research, namely TBM performance prediction, tunnelling-induced settlement prediction,  
5  
6 464 geological forecasting and cutterhead design optimisation. Many studies have reported the  
7  
8 465 successful application of machine learning techniques in tunnelling activities with high levels  
9  
10 466 of accuracy. The most popular methods adopted in the literature include artificial neural  
11  
12 467 networks, support vector machines/regression and fuzzy-based methods. A clear trend is  
13  
14 468 evident in the use of ML in tunnelling and this trend is likely to persist as the volume of data  
15  
16 469 produced by modern TBMs continues to grow and the use of machine learning becomes  
17  
18 470 more commonplace. In most instances, investigators have used empiricism (from previous  
19  
20 471 literature) as the basis for the selection of model inputs where the number of features varies  
21  
22 472 considerably across the literature. As the number of parameters captured by modern tunnel  
23  
24 473 boring machines grows, identification of the most appropriate features for training ML models  
25  
26 474 using robust techniques should be central to future research.

27  
28  
29  
30 475 Despite its recent advances, machine learning in tunnelling remains a young field with many  
31  
32 476 underexplored research opportunities. Some of these opportunities can be observed by  
33  
34 477 contrasting the methods reviewed in this study with those adopted in other disciplines such  
35  
36 478 as aerospace, healthcare, robotics, and automated vehicles (Mooney et al. 2020). In  
37  
38 479 particular, there is a real need for continued application of machine learning methods  
39  
40 480 employing more principled, probabilistic frameworks such as Bayesian networks and  
41  
42 481 Gaussian process regression. The problems covered by this review appear well-suited to  
43  
44 482 probabilistic frameworks given the uncertain nature of tunnelling operations and the  
45  
46 483 prevalence of noisy data. This relieves engineers of onerous data pre-processing to denoise  
47  
48 484 large training datasets. Furthermore, probabilistic frameworks provide a robust treatment of  
49  
50 485 overfitting meaning large datasets are not necessarily a prerequisite and deployment of  
51  
52 486 these techniques on a site-specific basis is feasible.

53  
54  
55  
56  
57  
58 487 Another important finding of this review is that most of the studies reviewed here have been  
59  
60 488 developed and validated against a single case history. Validation of these algorithms across

489 a broader parameter space are warranted for the industry to gain confidence in these  
1  
2 490 approaches. As tunnelling data becomes more accessible, it may also become feasible to  
3  
4 491 intelligently interrogate large datasets for the most appropriate training data for a given  
5  
6 492 project. This would allow the relative performance of machine learning techniques on future  
7  
8 493 projects to feedback into the improvement of the training datasets. In addition, the high-risk  
9  
10 nature of mistakes in the tunnelling industry means model interpretability is essential for  
11 494  
12 take-up in practice to gain insight into the features driving predictions.  
13 495  
14  
15

16 496 Graphical causal inference represents an exciting area for future research. Several authors  
17  
18 497 have argued that some of the most challenging open problems of machine learning and  
19  
20 artificial intelligence are intrinsically related to causality e.g. Pearl (2000, 2014), Schölkopf  
21 498 (2019). In particular, the machine learning models reviewed in this paper suffer from a lack  
22  
23 499 of generalisation (e.g. transfer to new problems). This is because these models are only  
24  
25 500 trained on the most relevant information to limit the associated computational cost. However,  
26  
27 501 information essential for generalisation, such as interventions, domain shifts, temporal  
28  
29 502 structure are typically neglected. Schölkopf (2019) argues that “causality, with its focus on  
30  
31 503 modelling and reasoning about interventions, can make a substantial contribution towards  
32  
33 504 understanding and resolving these issues and thus take the field to the next level”. The  
34  
35 505 integration of causal modelling in machine learning thus represents a promising avenue for  
36  
37 506 more robust treatment of uncertainty in practical domains. It appears essential for the  
38  
39 507 tunnelling industry to begin to consider how best to leverage these recent advances in  
40  
41 508 machine learning to inform tunnelling operations.  
42  
43 509  
44  
45  
46  
47  
48

49 510

## 52 511 REFERENCES

- 53  
54  
55 512 Acaroglu, O., Ozdemir, L. and Asbury, B., 2008. A fuzzy logic model to predict specific energy  
56 513 requirement for TBM performance prediction. *Tunnelling and Underground Space  
57 514 Technology*, 23(5), pp.600-608.  
58 515 Adoko, A.C., Jiao, Y.Y., Wu, L., Wang, H. and Wang, Z.H., 2013. Predicting tunnel convergence using  
59 516 multivariate adaptive regression spline and artificial neural network. *Tunnelling and  
60 517 Underground Space Technology*, 38, pp.368-376.  
61  
62  
63  
64  
65

- 518 Adoko, A.C., Gokceoglu, C. and Yagiz, S., 2017. Bayesian prediction of TBM penetration rate in rock  
 1 519 mass. *Engineering Geology*, 226, pp.245-256.
- 2 520 Adoko, A.C. and Yagiz, S., 2019. Fuzzy Inference System-Based for TBM Field Penetration Index  
 3 521 Estimation in Rock Mass. *Geotechnical and Geological Engineering*, 37(3), pp.1533-1553.
- 4 522 Ahangari, K., Moeinossadat, S.R. and Behnia, D., 2015. Estimation of tunnelling-induced settlement  
 5 523 by modern intelligent methods. *Soils and Foundations*, 55(4), pp.737-748.
- 6 524 Ahmed, N.K., Atiya, A.F., Gayar, N.E. and El-Shishiny, H., 2010. An empirical comparison of machine  
 7 525 learning models for time series forecasting. *Econometric Reviews*, 29(5-6), pp.594-621.
- 8 526 Alimoradi, A., Moradzadeh, A., Naderi, R., Salehi, M.Z. and Etemadi, A., 2008. Prediction of  
 9 527 geological hazardous zones in front of a tunnel face using TSP-203 and artificial neural  
 10 528 networks. *Tunnelling and Underground Space Technology*, 23(6), pp.711-717.
- 11 529 Armaghani, D.J., Mohamad, E.T., Narayanasamy, M.S., Narita, N. and Yagiz, S., 2017. Development  
 12 530 of hybrid intelligent models for predicting TBM penetration rate in hard rock  
 13 531 condition. *Tunnelling and Underground Space Technology*, 63, pp.29-43.
- 14 532 Armaghani, D.J., Faradonbeh, R.S., Momeni, E., Fahimifar, A. and Tahir, M.M., 2018. Performance  
 15 533 prediction of tunnel boring machine through developing a gene expression programming  
 16 534 equation. *Engineering with Computers*, 34(1), pp.129-141.
- 17 535 Armaghani, D.J., Koopialipoor, M., Marto, A. and Yagiz, S., 2019. Application of several optimization  
 18 536 techniques for estimating TBM advance rate in granitic rocks. *Journal of Rock Mechanics and  
 19 537 Geotechnical Engineering*, 11(4), pp.779-789.
- 20 538 Atashpaz-Gargari E and Lucas C (2007) Imperialist competitive algorithm: an algorithm for  
 21 539 optimization inspired by imperialistic competition. In *2007 IEEE congress on evolutionary  
 22 540 computation*, IEEE, pp. 4661-4667.
- 23 541 Barla, M., Camusso, M. and Aiassa, S. (2006). Analysis of jacking forces during microtunnelling in  
 24 542 limestone. *Tunnelling and Underground Space Technology*, 21(6):668-683.
- 25 543 Behnia, D. and Shahriar, K., 2015, November. Prediction of Tunnelling-induced Settlement Using  
 26 544 Gene Expression Programming. In *49th US Rock Mechanics/Geomechanics Symposium*.  
 27 545 American Rock Mechanics Association.
- 28 546 Benardos, A., 2008. Artificial intelligence in underground development: a study of TBM  
 29 547 performance. *Underground Spaces: Design, Engineering and Environmental Aspects*, 102,  
 30 548 p.121.
- 31 549 Benardos, A.G. and Kaliampakos, D.C., 2004. Modelling TBM performance with artificial neural  
 32 550 networks. *Tunnelling and Underground Space Technology*, 19(6), pp.597-605.
- 33 551 Bouayad, D. and Emeriault, F., 2014, May. Application of the hybrid ACP/ANFIS method for the  
 34 552 prediction of surface settlement induced by an earth pressure tunnel boring machine with  
 35 553 consideration of the encountered geology. In *NUMGE 2014 8th European Conference on  
 36 554 Numerical Methods in Geotechnical Engineering* (pp. 333-338). CRC Press.
- 37 555 Bouayad, D. and Emeriault, F., 2017. Modeling the relationship between ground surface settlements  
 38 556 induced by shield tunneling and the operational and geological parameters based on the hybrid  
 39 557 PCA/ANFIS method. *Tunnelling and Underground Space Technology*, 68, pp.142-152.
- 40 558 Bouayad, D., Emeriault, F. and Maza, M., 2015. Assessment of ground surface displacements  
 41 559 induced by an earth pressure balance shield tunneling using partial least squares  
 42 560 regression. *Environmental earth sciences*, 73(11), pp.7603-7616.
- 43 561 Boubou, R., Emeriault, F. and Kastner, R., 2010. Artificial neural network application for the prediction  
 44 562 of ground surface movements induced by shield tunnelling. *Canadian geotechnical  
 45 563 journal*, 47(11), pp.1214-1233.
- 46 564 Breiman, L., 2001. Random forests. *Machine learning*, 45(1), pp.5-32.
- 47 565 Brochu, E., Cora, V.M. and De Freitas, N., 2010. A tutorial on Bayesian optimization of expensive cost  
 48 566 functions, with application to active user modeling and hierarchical reinforcement  
 49 567 learning. *arXiv preprint arXiv:1012.2599*.
- 50 568 Cachim, P. and Bezuijen, A., 2019. Modelling the Torque with Artificial Neural Networks on a Tunnel  
 51 569 Boring Machine. *KSCE Journal of Civil Engineering*, 23(10), pp.4529-4537.
- 52 570 Cao, B.T., Freitag, S. and Meschke, G., 2016. A hybrid RNN-GPOD surrogate model for real-time  
 53 571 settlement predictions in mechanised tunnelling. *Advanced Modeling and Simulation in  
 54 572 Engineering Sciences*, 3(1), p.5.

- 573 Chen, R.P., Zhang, P., Kang, X., Zhong, Z.Q., Liu, Y. and Wu, H.N., 2019a. Prediction of maximum  
1 574 surface settlement caused by earth pressure balance (EPB) shield tunneling with ANN  
2 575 methods. *Soils and Foundations*, 59(2), pp.284-295.
- 3 576 Chen, R., Zhang, P., Wu, H., Wang, Z. and Zhong, Z., 2019b. Prediction of shield tunneling-induced  
4 577 ground settlement using machine learning techniques. *Frontiers of Structural and Civil  
5 578 Engineering*, 13(6), pp.1363-1378.
- 6 579 Chen, X., Li, X. and Zhu, H., 2019c. Condition evaluation of urban metro shield tunnels in Shanghai  
7 580 through multiple indicators multiple causes model combined with multiple regression  
8 581 method. *Tunnelling and Underground Space Technology*, 85, pp.170-181.
- 9 582 Chen, X., Zhu, H., Li, X., Lin, X. and Wang, X., 2019d. Probabilistic performance prediction of shield  
10 583 tunnels in operation through data mining. *Sustainable Cities and Society*, 44, pp.819-829.
- 11 584 Chieh, W.-C., Bai, X.-D., Sheil, B.B., Li, G. & Wang, F. (2020) Identifying characteristics of pipejacking  
12 585 parameters to assess geological conditions using optimisation algorithm-based support vector  
13 586 machines. *Tunnelling & Underground Space Technology*. In Press.
- 14 587 Choo, C.S. and Ong, D.E.L. (2015). Evaluation of pipe-jacking forces based on direct shear testing of  
15 588 reconstituted tunneling rock spoils. *Journal of Geotechnical and Geoenvironmental  
16 589 Engineering*, 141(10):04015044.
- 17 590 Darabi, A., Ahangari, K., Noorzad, A. and Arab, A., 2012. Subsidence estimation utilizing various  
18 591 approaches—A case study: Tehran No. 3 subway line. *Tunnelling and Underground Space  
19 592 Technology*, 31, pp.117-127.
- 20 593 Deng, J. (1982). Control problems of grey systems. *Systems and Control Letters*, 1, 288–294.
- 21 594 Dindarloo, S.R. and Siami-Irdemoosa, E., 2015. Maximum surface settlement based classification of  
22 595 shallow tunnels in soft ground. *Tunnelling and Underground Space Technology*, 49, pp.320-  
23 596 327.
- 24 597 Ding, H., Liu, S., Cai, S. and Xia, Y., 2019, September. Big Data Analysis of Structural Defects and  
25 598 Traffic Accidents in Existing Highway Tunnels. In *International Conference on Inforatmion  
26 599 technology in Geo-Engineering* (pp. 189-195). Springer, Cham.
- 27 600 J. C. Dunn (1973) A Fuzzy Relative of the ISODATA Process and Its Use in Detecting Compact Well-  
28 601 Separated Clusters, , 3:3, 32-57, DOI: 10.1080/01969727308546046
- 29 602 Erharter, G.H., Marcher, T. and Reinhold, C., 2019. Application of artificial neural networks for  
30 603 Underground construction—Chances and challenges—Insights from the BBT exploratory tunnel  
31 604 Ahrental Pfons. *Geomechanics and Tunnelling*, 12(5), pp.472-477.
- 32 605 Erharter, G.H., Marcher, T. and Reinhold, C., 2019, September. Artificial Neural Network Based  
33 606 Online Rockmass Behavior Classification of TBM Data. In *International Conference on  
34 607 Inforatmion technology in Geo-Engineering* (pp. 178-188). Springer, Cham.
- 35 608 Fattahi, H., 2016. Adaptive neuro fuzzy inference system based on fuzzy c-means clustering  
36 609 algorithm, a technique for estimation of TBM penetration rate. *Iran University of Science &  
37 610 Technology*, 6(2), pp.159-171.
- 38 611 Fattahi, H. and Babanouri, N., 2017. Applying optimized support vector regression models for  
39 612 prediction of tunnel boring machine performance. *Geotechnical and Geological  
40 613 Engineering*, 35(5), pp.2205-2217.
- 41 614 Fattahi, H. and Babanouri, N., 2018. RES-based model in evaluation of surface settlement caused by  
42 615 EPB shield tunneling. *Indian Geotechnical Journal*, 48(4), pp.746-752.
- 43 616 Fattahi, H. and Bayatzadehfard, Z., 2019. Forecasting Surface Settlement Caused by Shield  
44 617 Tunneling Using ANN-BBO Model and ANFIS Based on Clustering Methods. *Journal of  
45 618 Engineering Geology*, 12(5), pp.55-84.
- 46 619 Franza, A., Benardos, P.G. and Marshall, A.M., 2018. Use of artificial neural networks to analyse  
47 620 tunnelling-induced ground movements obtained from geotechnical centrifuge testing.
- 48 621 Gangrade, R. and Mooney, M., 2019. Incorporating Spatial Uncertainty into Site Investigations for  
49 622 Tunneling Applications. *Journal of Performance of Constructed Facilities*.
- 50 623 Gao, X., Shi, M., Song, X., Zhang, C. and Zhang, H., 2019. Recurrent neural networks for real-time  
51 624 prediction of TBM operating parameters. *Automation in Construction*, 98, pp.225-235.
- 52 625 Ge, Y., Wang, J. and Li, K., 2013. Prediction of hard rock TBM penetration rate using least square  
53 626 support vector machine. *IFAC Proceedings Volumes*, 46(13), pp.347-352.

- 627 Ghasemi, E., Yagiz, S. and Ataei, M., 2014. Predicting penetration rate of hard rock tunnel boring  
 1 628 machine using fuzzy logic. *Bulletin of Engineering Geology and the Environment*, 73(1), pp.23-  
 2 629 35.
- 3 630 Gholamnejad, J. and Tayarani, N., 2010. Application of artificial neural networks to the prediction of  
 4 631 tunnel boring machine penetration rate. *Mining Science and Technology (China)*, 20(5), pp.727-  
 5 632 733.
- 6 633 Goh, A.T. and Hefney, A.M., 2010. Reliability assessment of EPB tunnel-related settlement. *Geomech*  
 7 634 *Eng*, 2(1), pp.57-69.
- 8 635 Goh, A.T.C., Zhang, W., Zhang, Y., Xiao, Y. and Xiang, Y., 2018. Determination of earth pressure  
 9 636 balance tunnel-related maximum surface settlement: a multivariate adaptive regression splines  
 10 637 approach. *Bulletin of Engineering Geology and the Environment*, 77(2), pp.489-500.
- 11 638 Grasmick, J.G., Mooney, M.A., Trainor-Guitton, W.J. and Walton, G., 2020. Global versus Local  
 12 639 Simulation of Geotechnical Parameters for Tunneling Projects. *Journal of Geotechnical and*  
 13 640 *Geoenvironmental Engineering*, 146(7), p.04020048.
- 14 641 Grima, M.A., Bruines, P.A. and Verhoef, P.N.W., 2000. Modeling tunnel boring machine performance  
 15 642 by neuro-fuzzy methods. *Tunnelling and underground space technology*, 15(3), pp.259-269.
- 16 643 Guo, J., Ding, L., Luo, H., Zhou, C. and Ma, L., 2014. Wavelet prediction method for ground  
 17 644 deformation induced by tunneling. *Tunnelling and underground space technology*, 41, pp.137-  
 18 645 151.
- 19 646 Hajihassani, M., Abdullah, S.S., Asteris, P.G. and Armaghani, D.J., 2019. A gene expression  
 20 647 programming model for predicting tunnel convergence. *Applied Sciences*, 9(21), p.4650.
- 21 648 Hajihassani, M., Kalatehjari, R., Marto, A., Mohamad, H. and Khosrotash, M., 2020. 3D prediction of  
 22 649 tunneling-induced ground movements based on a hybrid ANN and empirical  
 23 650 methods. *Engineering with Computers*, 36(1), pp.251-269.
- 24 651 Hasanipanah, M., Noorian-Bidgoli, M., Armaghani, D.J. and Khamesi, H., 2016. Feasibility of PSO-  
 25 652 ANN model for predicting surface settlement caused by tunneling. *Engineering with*  
 26 653 *Computers*, 32(4), pp.705-715.
- 27 654 Hayashi, H., Miyanaka, M., Gomi, H., Tatsumi, J., Kawabe, N. and Shinji, M., 2019, September.  
 28 655 Prediction of Forward Tunnel Face Score of Rock Mass Classification for Stability by Applying  
 29 656 Machine Learning to Drilling Data. In *International Conference on Inforatmion technology in*  
 30 657 *Geo-Engineering* (pp. 268-278). Springer, Cham.
- 31 658 Holland JH (1992) *Adaptation in natural and artificial systems: an introductory analysis with*  
 32 659 *applications to biology, control, and artificial intelligence*. MIT press.
- 33 660 Hu, M., Li, W., Yan, K., Ji, Z. and Hu, H., 2019. Modern machine learning techniques for univariate  
 34 661 tunnel settlement forecasting: A comparative study. *Mathematical Problems in*  
 35 662 *Engineering*, 2019.
- 36 663 Huang, G.B., Zhu, Q.Y. and Siew, C.K., 2004, July. Extreme learning machine: a new learning  
 37 664 scheme of feedforward neural networks. In *2004 IEEE international joint conference on neural*  
 38 665 *networks (IEEE Cat. No. 04CH37541)* (Vol. 2, pp. 985-990). IEEE.
- 39 666 Huang, G.B., Zhu, Q.Y. and Siew, C.K., 2006. Extreme learning machine: theory and  
 40 667 applications. *Neurocomputing*, 70(1-3), pp.489-501.
- 41 668 Huang, G.B., Zhou, H., Ding, X. and Zhang, R., 2011. Extreme learning machine for regression and  
 42 669 multiclass classification. *IEEE Transactions on Systems, Man, and Cybernetics, Part B*  
 43 670 *(Cybernetics)*, 42(2), pp.513-529.
- 44 671 Huo, J., Sun, W., Chen, J., Su, P. and Deng, L., 2010. Optimal disc cutters plane layout design of the  
 45 672 full-face rock tunnel boring machine (tbm) based on a multi-objective genetic algorithm. *Journal*  
 46 673 *of Mechanical Science and Technology*, 24(2), pp.521-528.
- 47 674 Huo, J., Sun, W., Chen, J. and Zhang, X., 2011. Disc cutters plane layout design of the full-face rock  
 48 675 tunnel boring machine (TBM) based on different layout patterns. *Computers & industrial*  
 49 676 *engineering*, 61(4), pp.1209-1225.
- 50 677 Jang JSR, Suni CT and Mizutani E (1997) *Neuro-fuzzy and soft computing. A computational*  
 51 678 *approach to learning and machine intelligence*. Prentice Hall, New York, USA.
- 52 679 Ji, Z., Guo, B., Xia, Y. and Tang, L., 2016, August. TBM cutterhead structure optimization based on  
 53 680 sensitivity analysis. In *2016 12th IEEE/ASME International Conference on Mechatronic and*  
 54 681 *Embedded Systems and Applications (MESA)* (pp. 1-8). IEEE.

- 682 Jung, J.H., Chung, H., Kwon, Y.S. and Lee, I.M., 2019. An ANN to predict ground condition ahead of  
683 tunnel face using TBM operational data. *KSCE Journal of Civil Engineering*, 23(7), pp.3200-  
684 3206.
- 685 Kennedy J and Eberhart R (1995) Particle swarm optimization. In *Proceedings of ICNN95-  
686 International Conference on Neural Networks*. IEEE, vol. 4, pp. 1942-1948.
- 687 Khamesi, H., Torabi, S.R., Mirzaei-Nasirabad, H. and Ghadiri, Z., 2015. Improving the performance of  
688 intelligent back analysis for tunneling using optimized fuzzy systems: case study of the Karaj  
689 Subway Line 2 in Iran. *Journal of Computing in Civil Engineering*, 29(6), p.05014010.
- 690 Khatami, S.A., Mirhabibi, A., Khosravi, A. and Nahavandi, S., 2013, October. Artificial neural network  
691 analysis of twin tunnelling-induced ground settlements. In *2013 IEEE International Conference  
692 on Systems, Man, and Cybernetics* (pp. 2492-2497). IEEE.
- 693 Khetwal, S., Pei, S. and Gutierrez, M., 2019, September. A Data-Driven Approach for Direct  
694 Assessment and Analysis of Traffic Tunnel Resilience. In *International Conference on  
695 Inforatmion technology in Geo-Engineering* (pp. 168-177). Springer, Cham.
- 696 Kim, C.Y., Bae, G.J., Hong, S.W., Park, C.H., Moon, H.K. and Shin, H.S., 2001. Neural network based  
697 prediction of ground surface settlements due to tunnelling. *Computers and Geotechnics*, 28(6-  
698 7), pp.517-547.
- 699 Kohestani, V.R. and Bazarganlari-Lari, M.R. and Asgari-marnani, J. 2017. Prediction of maximum  
700 surface settlement caused by earth pressure balance shield tunneling using random  
701 forest. *Journal of AI and Data Mining*, 5(1), pp.127-135.
- 702 Kongsomboon, T., Suwansawat, S. and Sunthornjak, S., Predicting Ground Deformations Induced by  
703 Shield Tunneling Using Correlation Coefficient-ANN Technique. In *Proceedings of the World  
704 Tunnel Congress and 36<sup>th</sup> General Assembly*, Vancouver, Canada. Tunnelling association of  
705 Canada.
- 706 Koopialipoor, M., Nikouei, S.S., Marto, A., Fahimifar, A., Armaghani, D.J. and Mohamad, E.T., 2019a.  
707 Predicting tunnel boring machine performance through a new model based on the group  
708 method of data handling. *Bulletin of Engineering Geology and the Environment*, 78(5), pp.3799-  
709 3813.
- 710 Koopialipoor, M., Tootoonchi, H., Armaghani, D.J., Mohamad, E.T. and Hedayat, A., 2019b.  
711 Application of deep neural networks in predicting the penetration rate of tunnel boring  
712 machines. *Bulletin of Engineering Geology and the Environment*, 78(8), pp.6347-6360.
- 713 Koopialipoor, M., Fahimifar, A., Ghaleini, E.N., Momenzadeh, M. and Armaghani, D.J., 2020.  
714 Development of a new hybrid ANN for solving a geotechnical problem related to tunnel boring  
715 machine performance. *Engineering with Computers*, 36(1), pp.345-357.
- 716 Koukoutas, S.P. and Sofianos, A.I., 2015. Settlements due to single and twin tube urban EPB shield  
717 tunnelling. *Geotechnical and Geological Engineering*, 33(3), pp.487-510.
- 718 Kuo, Y., Yang, T. and Huang, G.W., 2008. The use of grey relational analysis in solving multiple  
719 attribute decision-making problems. *Computers & industrial engineering*, 55(1), pp.80-93.
- 720 Lai, J., Qiu, J., Feng, Z., Chen, J. and Fan, H., 2016. Prediction of soil deformation in tunnelling using  
721 artificial neural networks. *Computational Intelligence and Neuroscience*, 2016.
- 722 Li, S.J., Zhao, H.B. and Ru, Z.L., 2012. Deformation prediction of tunnel surrounding rock mass using  
723 CPSO-SVM model. *Journal of central south university*, 19(11), pp.3311-3319.
- 724 Li, X., Lin, X., Zhu, H., Wang, X. and Liu, Z., 2017. Condition assessment of shield tunnel using a new  
725 indicator: The tunnel serviceability index. *Tunnelling and Underground Space Technology*, 67,  
726 pp.98-106.
- 727 Ling, F., Jingcheng, W., Yang, G., Chuang, L. and Langwen, Z., 2013, May. Prediction of TBM  
728 penetration rate based on the model of PLS-FNN. In *2013 25th Chinese Control and Decision  
729 Conference (CCDC)* (pp. 1295-1299). IEEE.
- 730 Liu, Y. and Hou, S., 2019, September. Rockburst Prediction Based on Particle Swarm Optimization  
731 and Machine Learning Algorithm. In *International Conference on Inforatmion technology in  
732 Geo-Engineering* (pp. 292-303). Springer, Cham.
- 733 Liu, K. and Liu, B., 2019. Intelligent information-based construction in tunnel engineering based on the  
734 GA and CCGPR coupled algorithm. *Tunnelling and Underground Space Technology*, 88,  
735 pp.113-128.

- 736 Liu, B., Wang, R., Guan, Z., Li, J., Xu, Z., Guo, X. and Wang, Y., 2019. Improved support vector  
 1 737 regression models for predicting rock mass parameters using tunnel boring machine driving  
 2 738 data. *Tunnelling and Underground Space Technology*, 91, p.102958.
- 3 739 Liu, B., Wang, R., Zhao, G., Guo, X., Wang, Y., Li, J. and Wang, S., 2020. Prediction of rock mass  
 4 740 parameters in the TBM tunnel based on BP neural network integrated simulated annealing  
 5 741 algorithm. *Tunnelling and Underground Space Technology*, 95, p.103103.
- 6 742 Mahdevari, S. and Torabi, S.R., 2012. Prediction of tunnel convergence using artificial neural  
 7 743 networks. *Tunnelling and Underground Space Technology*, 28, pp.218-228.
- 8 744 Mahdevari, S., Torabi, S.R. and Monjezi, M., 2012. Application of artificial intelligence algorithms in  
 9 745 predicting tunnel convergence to avoid TBM jamming phenomenon. *International Journal of*  
 10 746 *Rock Mechanics and Mining Sciences*, 55, pp.33-44.
- 11 747 Mahdevari, S., Haghghat, H.S. and Torabi, S.R., 2013. A dynamically approach based on SVM  
 12 748 algorithm for prediction of tunnel convergence during excavation. *Tunnelling and underground*  
 13 749 *space technology*, 38, pp.59-68.
- 14 750 Mahdevari, S., Shahriar, K., Yagiz, S. and Shirazi, M.A., 2014. A support vector regression model for  
 15 751 predicting tunnel boring machine penetration rates. *International Journal of Rock Mechanics*  
 16 752 *and Mining Sciences*, 72, pp.214-229.
- 17 753 Maher, J., 2013. A Machine Learning Approach to Predicting and Maximizing Penetration Rates in  
 18 754 Earth Pressure Balance Tunnel Boring Machines. Report. Colorado School of Mines.
- 19 755 Martins, F.F. and Miranda, T.F., 2013. Prediction of hard rock TBM penetration rate based on Data  
 20 756 Mining techniques. In *18th International Conference on Soil Mechanics and Geotechnical*  
 21 757 *Engineering* (Vol. 2, pp. 1751-1754). Presses des Ponts.
- 22 758 Marto, A., Hajihassani, M., Kalatehjari, R., Namazi, E. and Sohaei, H., 2012. Simulation of longitudinal  
 23 759 surface settlement due to tunnelling using artificial neural network. *International Review on*  
 24 760 *Modelling and Simulations*, 5(2), pp.1024-1031.
- 25 761 Mehrnahad, H. and Zekrabad, M.K., 2018. Prediction of Tunnelling-Induced Surface Settlement with  
 26 762 Artificial Neural Networks, Case Study: Mashhad Subway Tunnel. *Journal of Engineering*  
 27 763 *Geology*, 12, p.135.
- 28 764 Mikaeil, R., Naghadehi, M.Z. and Sereshki, F., 2009. Multifactorial fuzzy approach to the penetrability  
 29 765 classification of TBM in hard rock conditions. *Tunnelling and Underground Space*  
 30 766 *Technology*, 24(5), pp.500-505.
- 31 767 Mikaeil, R., Naghadehi, M.Z. and Ghadernejad, S., 2018. An extended multifactorial fuzzy prediction  
 32 768 of hard rock TBM penetrability. *Geotechnical and Geological Engineering*, 36(3), pp.1779-1804.
- 33 769 Minh, V.T., Katushin, D., Antonov, M. and Veinthal, R., 2017. Regression models and fuzzy logic  
 34 770 prediction of TBM penetration rate. *Open Engineering*, 7(1), pp.60-68.
- 35 771 Mobarra, Y., Hajian, A. and Rezazadeh Anbarani, M., 2013. Application of Artificial Neural Networks  
 36 772 to the Prediction of TBM Penetration Rate in TBM-driven Golab Water Transfer Tunnel.  
 37 773 In *International Conference on Civil Engineering Architecture & Urban Sustainable*  
 38 774 *Development* (Vol. 27).
- 39 775 Moeinossadat, S.R. and Ahangari, K., 2019. Estimating maximum surface settlement due to EPBM  
 40 776 tunneling by Numerical-Intelligent approach—A case study: Tehran subway line  
 41 777 7. *Transportation Geotechnics*, 18, pp.92-102.
- 42 778 Moeinossadat, S.R., Ahangari, K. and Shahriar, K., 2018a. Control of ground settlements caused by  
 43 779 EPBS tunneling using an intelligent predictive model. *Indian Geotechnical Journal*, 48(3),  
 44 780 pp.420-429.
- 45 781 Moeinossadat, S.R., Ahangari, K. and Shahriar, K., 2018b. Modeling maximum surface settlement  
 46 782 due to EPBM tunneling by various soft computing techniques. *Innovative Infrastructure*  
 47 783 *Solutions*, 3(1), p.10.
- 48 784 Moghaddasi, M.R. and Noorian-Bidgoli, M., 2018. ICA-ANN, ANN and multiple regression models for  
 49 785 prediction of surface settlement caused by tunneling. *Tunnelling and Underground Space*  
 50 786 *Technology*, 79, pp.197-209.
- 51 787 Mohammadi, H., Farsangi, M.E., Rahmannedjad, R. and Poor, H.N., 2007. TBM Advance Rate  
 52 788 Prediction: An Artificial Neural Network Approach. In *Third National Congress in Civil*  
 53 789 *Engineering*, Tabriz, Iran.

- 790 Mohammadi, S.D., Naseri, F. and Alipoor, S., 2015. Development of artificial neural networks and  
1 791 multiple regression models for the NATM tunnelling-induced settlement in Niayesh subway tunnel,  
2 792 Tehran. *Bulletin of Engineering Geology and the Environment*, 74(3), pp.827-843.
- 3 793 Mokhtari, S. and Mooney, M.A., 2019. Feasibility study of EPB shield automation using deep learning.  
4 794 In *Tunnels and Underground Cities. Engineering and Innovation Meet Archaeology,*  
5 795 *Architecture and Art* (pp. 2691-2699). CRC Press.
- 6 796 Mokhtari, S., Navidi, W., and Mooney, M.A. White Box Regression (Elastic Net) Modeling of Earth  
7 797 Pressure Balance Shield Machine Advance Rate, *Automation in Construction*, 2020,  
8 798 115(103208).
- 9 799 Mokhtari, S. and Mooney, M.A., Predicting EPBM Advance Rate Performance using Support Vector  
10 800 Regression Modeling, *Tunnelling and Underground Space Technology*, 2020, in review.
- 11 801 Mooney MA, Yu H, Mokhtari S, Zhang X, and Zhou X. EPB TBM Performance Prediction on the  
12 802 University Link U230 Project. Proc. North American Tunneling Conference, Washington D.C.,  
13 803 June 24-27, 2018.
- 14 804 Mooney, M., Yu, H., Gangrade, R. EPB Shield TBM Automation using the Autonomous Vehicle  
15 805 Framework, Proc. North American Tunneling, Nashville, TN, June 7-10, 2020.
- 16 806 Naeini, S.A. and Khalili, A., 2017. Settlement Prediction for Tehran Subway Line-3 via FLAC3D and  
17 807 ANFIS. *International Journal of Geotechnical and Geological Engineering*, 11(7), pp.612-617.
- 18 808 Naghadehi, M.Z., Samaei, M. and Ranjbaria, M., Superior Modeling of Hard Rock TBM Performance  
19 809 Using Novel Predictive Analytics Methodologies.
- 20 810 Neaupane, K.M. and Adhikari, N.R., 2006. Prediction of tunneling-induced ground movement with the  
21 811 multi-layer perceptron. *Tunnelling and underground space technology*, 21(2), pp.151-159.
- 22 812 Ninic, J., Stascheit, J. and Meschke, G., 2011. Prediction of tunnelling induced settlements using  
23 813 simulation-based artificial neural networks. In *Proceedings of the Second International*  
24 814 *Conference on Soft Computing Technology in Civil, Structural and Environmental Engineering,*  
25 815 *page paper* (Vol. 26).
- 26 816 Ninić, J., Stascheit, J. and Meschke, G., 2013, September. Simulation-based steering for mechanized  
27 817 tunneling using an ANN-PSO-based meta-model. In *The Third International Conference on Soft*  
28 818 *Computing Technology in Civil, Structural and Environmental Engineering, Civil-Comp*  
29 819 *Press* (pp. 801-811).
- 30 820 O'Dwyer, K.G., McCabe, B.A., Sheil, B.B. and Herson, D.P. (2018). Blackpool South Strategy project:  
31 821 analysis of pipe-jacking records. *Proceedings of Civil Engineering Research in Ireland (CERI*  
32 822 *2018)*.
- 33 823 O'Dwyer, K.G., McCabe, B.A., Sheil, B.B. (2019). Interpretation of pipe-jacking and lubrication records  
34 824 for drives in silty soil. *Underground Space*. DOI: 10.1016/j.undsp.2019.04.001
- 35 825 Ocak, I. and Seker, S.E., 2013. Calculation of surface settlements caused by EPBM tunneling using  
36 826 artificial neural network, SVM, and Gaussian processes. *Environmental earth sciences*, 70(3),  
37 827 pp.1263-1276.
- 38 828 Oraee, K., Khorami, M.T. and Hosseini, N., 2012, February. Prediction of the penetration rate of TBM  
39 829 using adaptive neuro fuzzy inference system (ANFIS). In *Proceeding of SME annual meeting*  
40 830 *and exhibit, from the mine to the market, now it's global, Seattle, WA, USA* (pp. 297-302).
- 41 831 Pearl, J., 2000. Models, reasoning and inference. *Cambridge, UK: Cambridge University Press*.
- 42 832 Pearl, J., 2014. *Probabilistic reasoning in intelligent systems: networks of plausible inference*.  
43 833 Elsevier.
- 44 834 Phillips, B.M., Royston, R., Sheil, B.B. and Byrne, B.W. (2019) Instrumentation and monitoring of a  
45 835 concrete jacking pipe. In *International Conference on Smart Infrastructure and Construction*  
46 836 *(ICSIC)*, Cambridge.
- 47 837 Pourtaghi, A. and Lotfollahi-Yaghin, M.A., 2012. Wavenet ability assessment in comparison to ANN  
48 838 for predicting the maximum surface settlement caused by tunneling. *Tunnelling and*  
49 839 *Underground Space Technology*, 28, pp.257-271.
- 50 840 Qi, G., Zhengying, W., Jun, D.U. and Yiping, T., 2013, September. A cutter layout optimization  
51 841 method for full-face rock tunnel boring machine. In *International Conference on Intelligent*  
52 842 *Robotics and Applications* (pp. 727-737). Springer, Berlin, Heidelberg.

- 843 Qiao, J., Liu, J., Guo, W. and Zhang, Y., 2010, November. Artificial neural network to predict the  
1 844 surface maximum settlement by shield tunneling. In *International Conference on Intelligent  
2 845 Robotics and Applications* (pp. 257-265). Springer, Berlin, Heidelberg.
- 3 846 Rafiai, H. and Moosavi, M., 2012. An approximate ANN-based solution for convergence of lined  
4 847 circular tunnels in elasto-plastic rock masses with anisotropic stresses. *Tunnelling and  
5 848 Underground Space Technology*, 27(1), pp.52-59.
- 6 849 Ramezanshirazi, M., Sebastiani, D. and Miliziano, S., 2019, July. Artificial Intelligence to Predict  
7 850 Maximum Surface Settlements Induced by Mechanized Tunnelling. In *National Conference of  
8 851 the Researchers of Geotechnical Engineering* (pp. 490-499). Springer, Cham.
- 9 852 Rostami, J. and Chang, S.H., 2017. A closer look at the design of cutterheads for hard rock tunnel-  
10 853 boring machines. *Engineering*, 3(6), pp.892-904.
- 11 854 Royston, R., Sheil, B.B. & Byrne, B.W. (2020) Monitoring the construction of a large-diameter caisson  
12 855 in sand. *Proceedings of the ICE - Geotechnical Engineering*. Published online, DOI:  
13 856 10.1680/jgeen.19.00266.
- 14 857 Royston, R., Sheil, B.B. & Byrne, B.W. (2020) Undrained bearing capacity of the cutting face of large-  
15 858 diameter caissons. *Géotechnique*. In press.
- 16 859 Saadallah, A., Egorov, A., Cao, B.T., Freitag, S., Morik, K. and Meschke, G., 2019. Active learning for  
17 860 accurate settlement prediction using numerical simulations in mechanized tunneling. *Procedia  
18 861 CIRP*, 81, pp.1052-1058.
- 19 862 Salimi, A. and Esmaeili, M., 2013. Utilising of linear and non-linear prediction tools for evaluation of  
20 863 penetration rate of tunnel boring machine in hard rock condition. *International Journal of Mining  
21 864 and Mineral Engineering*, 4(3), pp.249-264.
- 22 865 Salimi, A., Moormann, C., Singh, T. and Jain, P., 2015, November. TBM performance prediction in  
23 866 rock tunneling using various artificial intelligence algorithms. In *11th Iranian and 2nd regional  
24 867 tunnelling conference Iran*.
- 25 868 Salimi, A., Rostami, J., Moormann, C. and Delisio, A., 2016. Application of non-linear regression  
26 869 analysis and artificial intelligence algorithms for performance prediction of hard rock  
27 870 TBMs. *Tunnelling and Underground Space Technology*, 58, pp.236-246.
- 28 871 Salimi, A., Rostami, J. and Moormann, C., 2019. Application of rock mass classification systems for  
29 872 performance estimation of rock TBMs using regression tree and artificial intelligence  
30 873 algorithms. *Tunnelling and Underground Space Technology*, 92, p.103046.
- 31 874 Santos Jr, O.J. and Celestino, T.B., 2008. Artificial neural networks analysis of Sao Paulo subway  
32 875 tunnel settlement data. *Tunnelling and underground space technology*, 23(5), pp.481-491.
- 33 876 Schaeffer, K. and Mooney, M.A. Examining the Influence of TBM-Ground Interaction on Electrical  
34 877 Resistivity Imaging ahead of the TBM, *Tunnelling & Underground Space Technology*, 2016, 58  
35 878 (82-98).
- 36 879 Schölkopf, B., 2019. Causality for machine learning. *arXiv preprint arXiv:1911.10500*.
- 37 880 Shao, C., Li, X. and Su, H., 2013, September. Performance prediction of hard rock TBM based on  
38 881 extreme learning machine. In *International Conference on Intelligent Robotics and  
39 882 Applications* (pp. 409-416). Springer, Berlin, Heidelberg.
- 40 883 Sheil, B.B., Curran, B.G. and McCabe, B.A. (2016). Experiences of utility microtunnelling in Irish  
41 884 limestone, mudstone and sandstone rock. *Tunnelling and Underground Space  
42 885 Technology*, 51:326-337.
- 43 886 Sheil, B., Royston, R. and Byrne, B., 2018. Real-Time Monitoring of Large-Diameter Caissons.  
44 887 In *Proceedings of China-Europe Conference on Geotechnical Engineering* (pp. 725-729).  
45 888 Springer.
- 46 889 Sheil, B.B., Suryasentana, S. and Cheng, W.-C. (2020) An assessment of anomaly detection methods  
47 890 applied to microtunnelling. *Journal of Geotechnical and Geoenvironmental Engineering*. In  
48 891 press.
- 49 892 Shi, J., Ortigao, J.A.R. and Bai, J., 1998. Modular neural networks for predicting settlements during  
50 893 tunneling. *Journal of Geotechnical and Geoenvironmental Engineering*, 124(5), pp.389-395.
- 51 894 Shi, M., Zhang, L., Sun, W. and Song, X., 2019a. A fuzzy c-means algorithm guided by attribute  
52 895 correlations and its application in the big data analysis of tunnel boring machine. *Knowledge-  
53 896 Based Systems*, 182, p.104859.

- 897 Shi, S., Zhao, R., Li, S., Xie, X., Li, L., Zhou, Z. and Liu, H., 2019b. Intelligent prediction of  
1 898 surrounding rock deformation of shallow buried highway tunnel and its engineering  
2 899 application. *Tunnelling and Underground Space Technology*, 90, pp.1-11.
- 3 900 Simoes, M.G. and Kim, T., 2006. Fuzzy modeling approaches for the prediction of machine utilization  
4 901 in hard rock tunnel boring machines. In *Conference record of the 2006 IEEE industry  
5 902 applications conference forty-first IAS annual meeting* (Vol. 2, pp. 947-954). IEEE.
- 6 903 Song, X., Shi, M., Wu, J. and Sun, W., 2019. A new fuzzy c-means clustering-based time series  
7 904 segmentation approach and its application on tunnel boring machine analysis. *Mechanical  
8 905 Systems and Signal Processing*, 133, p.106279.
- 9 906 Špačková, O. and Straub, D., 2013. Dynamic Bayesian network for probabilistic modeling of tunnel  
10 907 excavation processes. *Computer-Aided Civil and Infrastructure Engineering*, 28(1), pp.1-21.
- 11 908 Sun, Y., Feng, X. and Yang, L., 2018a. Predicting tunnel squeezing using multiclass support vector  
12 909 machines. *Advances in Civil Engineering*, 2018.
- 13 910 Sun, W., Shi, M., Zhang, C., Zhao, J. and Song, X., 2018b. Dynamic load prediction of tunnel boring  
14 911 machine (TBM) based on heterogeneous in-situ data. *Automation in Construction*, 92, pp.23-  
15 912 34.
- 16 913 Suwansawat, S. and Einstein, H.H., 2006. Artificial neural networks for predicting the maximum  
17 914 surface settlement caused by EPB shield tunneling. *Tunnelling and underground space  
18 915 technology*, 21(2), pp.133-150.
- 19 916 Takagi, T. and Sugeno, M., 1985. Fuzzy identification of systems and its applications to modeling and  
20 917 control. *IEEE transactions on systems, man, and cybernetics*, (1), pp.116-132.
- 21 918 Tao, H., Jingcheng, W. and Langwen, Z., 2015, May. Prediction of hard rock TBM penetration rate  
22 919 using random forests. In *The 27th Chinese Control and Decision Conference (2015 CCDC)* (pp.  
23 920 3716-3720). IEEE.
- 24 921 Tsekouras, G.J., Koukoulis, J. and Mastorakis, N.E., 2010. An optimized neural network for predicting  
25 922 settlements during tunneling excavation. *WSEAS TRANSACTIONS on SYSTEMS*, 9(12),  
26 923 pp.1153-1167.
- 27 924 Vapnik, V. "The nature of statistical learning theory," Springer-Verlag: New York, 1995.
- 28 925 Von, W.C. and Ismail, M.A.M., 2017, October. Evaluation of tunnel seismic prediction (TSP) result  
29 926 using the Japanese highway rock mass classification system for Pahang-Selangor Raw Water  
30 927 Transfer Tunnel. In *AIP Conference Proceedings* (Vol. 1892, No. 1, p. 030011). AIP Publishing  
31 928 LLC.
- 32 929 Wang, F., Gou, B., Zhang, Q., Qin, Y. and Li, B., 2016. Evaluation of ground settlement in response to  
33 930 shield penetration using numerical and statistical methods: a metro tunnel construction  
34 931 case. *Structure and Infrastructure Engineering*, 12(9), pp.1024-1037.
- 35 932 Wang, C., Osorio-Murillo, C.A., Zhu, H. and Rubin, Y., 2017. Bayesian approach for calibrating  
36 933 transformation model from spatially varied CPT data to regular geotechnical  
37 934 parameter. *Computers and Geotechnics*, 85, pp.262-273.
- 38 935 Wei, L., Magee, D.R. and Cohn, A.G., 2018. An anomalous event detection and tracking method for a  
39 936 tunnel look-ahead ground prediction system. *Automation in Construction*, 91, pp.216-225.
- 40 937 Williams, C.K. and Rasmussen, C.E., 1996. Gaussian processes for regression. In *Advances in  
41 938 neural information processing systems* (pp. 514-520).
- 42 939 Xia, Y.M., Wu, F., Cheng, L. and Zhang, Z.H., 2012. Optimal Design of Disc Cutter Structure  
43 940 Parameter Based on Genetic Algorithm. In *Applied Mechanics and Materials* (Vol. 130, pp. 919-  
44 941 922). Trans Tech Publications Ltd.
- 45 942 Xia, Y., Zhang, K., and Liu, J. 2015. Design optimization of TBM disc cutters for different geological  
46 943 conditions. *World journal of engineering and technology*, 3(4).
- 47 944 Xu, H., Zhou, J., G Asteris, P., Jahed Armaghani, D. and Tahir, M.M., 2019. Supervised machine  
48 945 learning techniques to the prediction of tunnel boring machine penetration rate. *Applied  
49 946 Sciences*, 9(18), p.3715.
- 50 947 Xue, Y.D. and Zhang, S., 2019, September. A Fast Metro Tunnel Profile Measuring Method Based on  
51 948 Close-Range Photogrammetry. In *International Conference on Inforatmion technology in Geo-  
52 949 Engineering* (pp. 57-69). Springer, Cham.

- 950 Yagiz, S., Gokceoglu, C., Sezer, E. and Iplikci, S., 2009. Application of two non-linear prediction tools  
 1 951 to the estimation of tunnel boring machine performance. *Engineering Applications of Artificial*  
 2 952 *Intelligence*, 22(4-5), pp.808-814.
- 3 953 Yagiz, S. and Karahan, H., 2011. Prediction of hard rock TBM penetration rate using particle swarm  
 4 954 optimization. *International Journal of Rock Mechanics and Mining Sciences*, 48(3), pp.427-433.
- 5 955 Yagiz, S. and Karahan, H., 2015. Application of various optimization techniques and comparison of  
 6 956 their performances for predicting TBM penetration rate in rock mass. *International Journal of*  
 7 957 *Rock Mechanics and Mining Sciences*, 80, pp.308-315.
- 8  
 9 958 Yamamoto, T., Shirasagi, S., Yamamoto, S., Mito, Y. and Aoki, K., 2003. Evaluation of the geological  
 10 959 condition ahead of the tunnel face by geostatistical techniques using TBM driving  
 11 960 data. *Tunnelling and underground space technology*, 18(2-3), pp.213-221.
- 12 961 Yan, K., Dai, Y., Xu, M. and Mo, Y., 2020. Tunnel Surface Settlement Forecasting with Ensemble  
 13 962 Learning. *Sustainability*, 12(1), p.232.
- 14 963 Yu, Y., Workman, A., Grasmick, J.G., Mooney, M.A. and Hering, A.S., 2018. Space-time outlier  
 15 964 identification in a large ground deformation data set. *Journal of Quality Technology*, 50(4),  
 16 965 pp.431-445.
- 17  
 18 966 Yu, H.J. and Mooney, M.A., Logging the As-Encountered Ground Condition with EPBM Data using  
 19 967 Supervised and Semi-Supervised Learning, *Tunnelling & Underground Space Technology*,  
 20 968 2020, in review.
- 21 969 Zhang, W., 2020. MARS Use for Determination of EPB Tunnel-Related Maximum Surface Settlement.  
 22 970 In *MARS Applications in Geotechnical Engineering Systems* (pp. 121-136). Springer,  
 23 971 Singapore.
- 24 972 Zhang L, Wu X, Qin Y, et al. 2016. Towards a fuzzy Bayesian network based approach for safety risk  
 25 973 analysis of tunnel-induced pipeline damage. *Risk Analysis*, 36(2): 278-301.
- 26 974 Zhang, L., Wu, X., Ji, W. and AbouRizk, S.M., 2017. Intelligent approach to estimation of tunnel-  
 27 975 induced ground settlement using wavelet packet and support vector machines. *Journal of*  
 28 976 *Computing in Civil Engineering*, 31(2), p.04016053.
- 29  
 30 977 Zhang, P., Chen, R.P. and Wu, H.N., 2019a. Real-time analysis and regulation of EPB shield steering  
 31 978 using Random Forest. *Automation in Construction*, 106, p.102860.
- 32 979 Zhang, L., Wu, X., Liu, W. and Skibniewski, M.J., 2019b. Optimal Strategy to Mitigate Tunnel-Induced  
 33 980 Settlement in Soft Soils: Simulation Approach. *Journal of Performance of Constructed*  
 34 981 *Facilities*, 33(5), p.04019058.
- 35 982 Zhang, Q., Liu, Z. and Tan, J., 2019c. Prediction of geological conditions for a tunnel boring machine  
 36 983 using big operational data. *Automation in Construction*, 100, pp.73-83.
- 37  
 38 984 Zhang, W.G., Li, H.R., Wu, C.Z., Li, Y.Q., Liu, Z.Q. and Liu, H.L., 2020. Soft computing approach for  
 39 985 prediction of surface settlement induced by earth pressure balance shield  
 40 986 tunneling. *Underground Space*.
- 41 987 Zhao, Z., Gong, Q., Zhang, Y. and Zhao, J., 2007. Prediction model of tunnel boring machine  
 42 988 performance by ensemble neural networks. *Geomechanics and Geoengineering: An*  
 43 989 *International Journal*, 2(2), pp.123-128.
- 44 990 Zhao, J., Shi, M., Hu, G., Song, X., Zhang, C., Tao, D. and Wu, W., 2019a. A Data-Driven Framework  
 45 991 for Tunnel Geological-Type Prediction Based on TBM Operating Data. *IEEE Access*, 7,  
 46 992 pp.66703-66713.
- 47  
 48 993 Zhao, W., Wei, Y., Liu, B., Liu, S. and Xiao, L., 2019b, September. Design and Application of  
 49 994 Automatic Monitoring and BIM Technology to the Construction of Shield-Bored Underneath  
 50 995 Building. In *International Conference on Inforatmion technology in Geo-Engineering* (pp. 493-  
 51 996 501). Springer, Cham.
- 52 997 Zhou, J., Shi, X.Z., Du, K., Qiu, X.Y., Li, X.B. and Mitri, H.S., 2016, July. Development of the ground  
 53 998 movements due to shield tunnelling prediction model using random forests. In Proc., 4th Geo-  
 54 999 China Int. Conf (pp. 108-115).
- 55 1000 Zhou, J., Shi, X., Du, K., Qiu, X., Li, X. and Mitri, H.S., 2017. Feasibility of random-forest approach for  
 56 1001 prediction of ground settlements induced by the construction of a shield-driven  
 57 1002 tunnel. *International Journal of Geomechanics*, 17(6), p.04016129.

1003 Zhou, J., Bejarbaneh, B.Y., Armaghani, D.J. and Tahir, M.M., 2019. Forecasting of TBM advance rate  
1 1004 in hard rock condition based on artificial neural network and genetic programming  
2 1005 techniques. *Bulletin of Engineering Geology and the Environment*, pp.1-16.

3 1006 Zhu M, Zhu H, Wang X, et al. Quantitative Analysis of Seasonal Uncertainty of Metro Tunnel's Long-  
4 1007 Term Longitudinal Settlement via Hierarchy Bayesian Network. In Proc. International  
5 1008 Conference on Information technology in Geo-Engineering. Springer, Cham, 2019: 279-291.

6 1009 Zhu, M., Zhu, H., Guo, F., Chen, X. and Ju, J.W. (2020). Tunnel condition assessment via cloud  
7 1010 model-based random forests and self-training approach. *Computer-Aided Civil and*  
8 1011 *Infrastructure Engineering*. In press.

9 1012 Zhuang, D.Y., Ma, K., Tang, C.A., Liang, Z.Z., Wang, K.K. and Wang, Z.W., 2019. Mechanical  
10 1013 parameter inversion in tunnel engineering using support vector regression optimized by multi-  
11 1014 strategy artificial fish swarm algorithm. *Tunnelling and Underground Space Technology*, 83,  
12 1015 pp.425-436.

14  
15  
16  
17  
18  
19  
20  
21  
22  
23  
24  
25  
26  
27  
28  
29  
30  
31  
32  
33  
34  
35  
36  
37  
38  
39  
40  
41  
42  
43  
44  
45  
46  
47  
48  
49  
50  
51  
52  
53  
54  
55  
56  
57  
58  
59  
60  
61  
62  
63  
64  
65

**Table 1** Summary of previous studies exploring the application of ML algorithms to the prediction of TBM performance

Reference	ML algorithm <sup>a</sup>	Features <sup>b</sup>	Predictand <sup>c</sup>	TBM type <sup>d</sup>	Dataset and size
Grima et al. (2000)	ANFIS	Core fracture frequency, UCS, RPMthrust/cutter, $D_c$	PR	-	640 - various tunnels worldwide
Bernardos & Kaliampakos (2004)	ANN (8-9-4-1)	Rock mass fracture degree, RMW, SF, RMQ, UCS, H, WT, k	AR	O	11 - Athens metro tunnel (Greece)
Simoies & Kim (2006)	Fuzzy logic (rule- and parametric-based)	D, RQD, RMR, water inflow rate	Utilization	O	Milyang tunnel (South Korea) Queens water tunnel (USA) Manapouri tunnel (New Zealand)
Mohammadi et al. (2007)	RBF-ANN (8-?-1)	RQD, UCS, SF, WT, RMW, RMR, H, k	AR	O	11 - Athens metro tunnel (Greece)
Zhao et al. (2007)	Ensemble neural network	UCS, DPW, $\alpha$ , BI	SBI	EPB	47 - The Deep Tunnel Sewerage System (Singapore)
Acaroglu et al. (2008)	Fuzzy logic	UCS, BTS, $D_c$ , $t_c$ , $s_c$ , penetration	SER	-	Linear cutting tests
Bernardos (2008)	ANN (8-9-5-1); ANN (8-9-4-1)	RQD, RMW, SF, RMR, UCS, H, WT, k	PR	O	330 - Maen tunnel 301 - Pieve tunnel (Italy) 11 - Athens metro tunnel (Greece)
Mikaeil et al. (2009)	Multifactorial fuzzy evaluation	UCS, BTS, PSI, DPW, $\alpha$	PR	O	151 - Queens water tunnel (USA)
Yagiz et al. (2009)	ANN (4-8-1); non-linear multivariate regression	UCS, BI, DPW, $\alpha$	PR	O	151 - Queens water tunnel (USA)
Gholamnejad & Tayarani (2010)	ANN (3-9-7-3-1)	UCS, RQD, DPW	PR	O	185 - Queens water tunnel (USA), Karaj-Tehran water tunnel (Iran), Gilgel Gibe II tunnel (Ethiopia)
Yagiz & Karahan (2011)	PSO	UCS, BI, DPW, $\alpha$ , TBM field data	PR	O	151 - Queens water tunnel (USA)
Maher (2013)	Linear regression; Polynomial regression (degree = 3); SVR (linear, polynomial kernels)	12 TBM parameters	PR	EPB	Seattle subway tunnel (USA)
Oraee et al. (2012)	ANFIS	RQD, UCS, DPW	PR	O	177 - Queens water tunnel (USA), Gilgel Gibe II tunnel (Ethiopia)
Ge et al. (2013)	Least squares SVM	UCS, BTS, PSI, DPW, $\alpha$	PR	O	151 - Queens water tunnel (USA)
Ling et al. (2013)	Partial least squares FNN	UCS, BTS, PSI, DPW, $\alpha$	PR	O	151 - Queens water tunnel (USA)
Martins & Miranda (2013)	ANN (4-2-1) SVR (RBF kernel)	UCS, PSI, DPW, $\alpha$	PR	O	151 - Queens water tunnel (USA)
Mobarra et al. (2013)	ANN (4-13-4-1)	UCS, PLS, RPM, normal force designation	PR	O	289 - Golab water tunnel (Iran)

Salimi & Esmaeili (2013)	Linear regression Non-linear multiple regression ANN (5-17-10-1)	UCS, BTS, PSI, DPW, $\alpha$	PR	O	46 - Karaj-Tehran water tunnel (Iran)
Shao et al. (2013)	Online prediction with ELM incremental learning	UCS, BTS, PSI, DPW, $\alpha$	PR	O	151 - Queens water tunnel (USA)
Špačková & Straub (2013)	Dynamic Bayesian networks	Ground zone, rock class, H, ground class, human factor, project geometry, CM, failure mode, number of failures	Time	-	Numerical modelling of Suncheon-Dolsan tunnel (South Korea)
Ghasemi et al. (2014)	Fuzzy logic	UCS, BTS, BI, DPW, $\alpha$	PR	O	151 - Queens water tunnel (USA)
Mahdevari et al. (2014)	SVR (RBF kernel)	JF, $\alpha$ , UCS, BTS, CP, DPW, SE, BI	PR	O	151 - Queens water tunnel (USA)
Salimi et al. (2015)	ANN (2-4-1); ANFIS; SVR (RBF kernel)	UCS, DPW	PR	O	75 - Zagros water conveyance tunnel (Iran)
Tao et al. (2015)	RF	UCS, BTS, BI, DPW, $\alpha$	PR	O	151 - Queens water tunnel (USA)
Yagiz & Karahan (2015)	DE				
Yagiz & Karahan (2015)	Hybrid harmony search	UCS, BI, DPW, $\alpha$	PR	O	151 - Queens water tunnel (USA)
Fattahi (2016)	Grey wolf optimiser				
Fattahi (2016)	FCM-ANFIS	UCS, BI, DPW, $\alpha$	PR	O	151 - Queens water tunnel (USA)
Salimi et al. (2016)	ANFIS				
Salimi et al. (2016)	SVR (RBF kernel)	UCS, DPW	PR	O	75 - Zagros water conveyance tunnel (Iran)
Adoko et al. (2017)	Bayesian inference	UCS, BI, DPW, $\alpha$	PR	O	151 - Queens water tunnel (USA)
Armaghani et al. (2017)	ANN (7-11-1); PSO-AAN (7-11-1); ICA-ANN (7-11-1)	UCS, BI, RQD, RMR, RMW, JF, RPM	PR	O	1286 - PSRWT tunnel (Malaysia)
Fattahi & Babanouri (2017)	DE-SVM; artificial bee colony				
Fattahi & Babanouri (2017)	SVM; Gravitational search SVM	UCS, BI, DPW, $\alpha$	PR	O	151 - Queens water tunnel (USA)
Minh et al. (2017)	Fuzzy logic	UCS, BTS, BI, DPW, $\alpha$	PR	O	151 - Queens water tunnel (USA)
Mooney et al. (2018)	SVR (RBF kernel); RRelief feature selection)	JF, CP, $Q_F$ , H, $H_w$	AR	EPB	Seattle University link tunnel (USA)
Armaghani et al. (2018)	GEP	UCS, BTS, RQD, RMR, RMW, JF, RPM	PR	O	1286 - PSRWT tunnel (Malaysia)
Mikaeil et al. (2018)	Multifactorial fuzzy evaluation approach	UCS, PSI, DPW, $\alpha$	PR	O	151 - Queens water tunnel (USA)
Adoko & Yagiz (2019)	FCM clustering; Subtractive clustering; ANFIS; Knowledge-based fuzzy inference	Rock type, UCS, BI, $\alpha$ , DPW, JF	FPI	O	151 - Queens water tunnel (USA)
Armaghani et al. (2019)	PSO-ANN (8-12-1); ICA-ANN (8-12-1)	UCS, BTS, RMR, RQD, q, RMW, JF, RPM	AR	O	1286 - PSRWT tunnel (Malaysia)
Cachim & Bezuijen (2019)	Time series ANN	Foam injection ratio, lagged values of torque	T	EPB	Botlek rail tunnel (Netherlands)

Gao et al. (2019)	RNN; Long-short term memory networks; Gated recurrent networks.	44 TBM parameters	T, velocity, JF, $P_c$	EPB	Shenzhen subway tunnel (China)
Koopialipoor et al. (2019a)	Group method of data handling	UCS, BTS, RQD, RMR, RMW, JF, RPM	PR	O	1286 - PSRWT tunnel (Malaysia)
Koopialipoor et al. (2019b)	ANN (5-8-32-8-1)	UCS, BTS, RQD, RMR, RMW	PR	O	1286 - PSRWT tunnel (Malaysia)
Naghadehi et al. (2019)	ICA-GEP	UCS, BTS, BI, DPW, $\alpha$	PR	O	151 - Queens water tunnel (USA)
Salimi et al. (2019)	CART; GP	UCS, RQD, DPW, joint condition	FPI	-	Various tunnels worldwide
Shi et al. (2019a)	FCM clustering; Attribute correlation guided FCM clustering	53 TBM parameters	PR	EPB	Tunnel in China
Song et al. (2019)	Time series segmentation guided by FCM clustering	53 TBM parameters	PR	EPB	Tunnel in China
Xu et al. (2019)	$kNN$ ; SVR (RBF kernels); ANN (6-?-1); CART; Chi-squared automatic	UCS, BTS, RQD, RMW, JF, RPM	PR	O	1286 - PSRWT tunnel (Malaysia)
Zhou et al. (2019)	ANN (6-2-1); GP	UCS, RQD, RMR, BTS, JF, RPM	AR	O	1286 - PSRWT tunnel (Malaysia)
Koopialipoor et al. (2020)	Hybrid firefly-ANN (7-8-1)	UCS, BTS, RQD, RMR, RMW, JF, RPM	PR	O	1286 - PSRWT tunnel (Malaysia)
Mokhtari et al. (2020)	Elastic net regression	RPM, JF, $Q_F$ , CP, SCP, H	AR	EPB	Seattle Northlink Extension tunnel (USA)
Mokhtari & Mooney (2020)	SVR (RBF kernel); RReliefF feature selection	RPM, JF, $Q_F$ , CP, SCP	AR	EPB	Seattle Northlink Extension tunnel (USA)

<sup>a</sup>FNN = fuzzy neural networks,  $kNN$  = k-nearest neighbours; <sup>b</sup>CM= construction method, CP = cutterhead power, RPM = cutterhead rotation speed, SE = specific energy, SF = stability factor, JF = cutterhead jacking force,  $Q_F$  = conditioning foam flow rate, SCP = screw conveyor power, H = cover from surface to TBM,  $H_w$  = height of groundwater table above TBM; <sup>c</sup>PR = penetration rate, AR = advance rate, SBI = specific rock mass boreability index, SER = specific energy requirement, FPI = field penetration index. <sup>d</sup>EPB = earth pressure balance, O = open mode hard rock.



**Table 2** Definition of rock parameters used in Table 1

<b>Parameter</b>	<b>Definition</b>
UCS	Unconfined compressive strength
DPW	Distance between planes of weakness
$\alpha$	Joint orientation
BTS	Brazilian tensile strength
BI	Brittleness index
RQD	Rock quality designation
RMW	Rock mass weathering
RMR	Rock mass rating
PSI	Point strength index
RMQ	Rock mass quality
q	Quartz content
PLS	Point load strength

**Table 3** Summary of previous studies exploring the application of ML algorithms to the prediction of tunnel-induced settlements

Reference	ML algorithm <sup>a</sup>	Salient features <sup>b</sup>	Predictand <sup>c</sup>	Dataset and size
Shi et al. (1998)	ANN (8-24-1)	$L, H, A$ , delay in closing inverted arch, WT, AR, CM, SPT values	$S_{max}$	356 – Brasilia tunnel (Brazil)
Kim et al. (2001)	ANN (47-47-47-47-2)	47 tunnel, TBM & soil parameters	$S_{max}, i$	113 – Seoul subway tunnel (South Korea)
Neaupane & Adhukari (2006)	ANN (6-3-9-1)	$H, D, s_u, V_L, CM, WT$	$S_{max}$	26 – various projects worldwide
Neaupane & Adhukari (2006)	ANN (6-3-5-1)	$H, D, s_u, V_L, CM, WT, S_{max}$	$U_{max}$	26 – various projects worldwide
Sunsawat & Einstein (2006)	ANN (10-20-1)	$H, L$ , geology @ crown & invert, WT, $P_t, PR, \theta, P_g, V_g$	$S_{max}$	49 – Bangkok MRTA tunnel (Thailand)
Yoo & Kim (2007)	ANN (8-4-4)	$H, WT$ , support pattern, geologies, soil layer thicknesses	$S_{max}, C$ , lining stresses	95 – high speed railway tunnel (South Korea)
Santos & Celestino (2008)	ANN (14-12-6-1)	14 parameters: tunnel geometry & ground conditions	$S_{max}$	81 – Sao Paulo subway tunnel (Brazil)
Boubou et al. (2010)	ANN (11-7-7-1)	AR, T, $P_t, P_g, V_g, JF$ , time, steering deviations, total work, $X/H$	$S(X)$	432 – Toulouse subway tunnel (France)
Franza et al. (2010)	ANN (5-4-2)	$H, R_d, V_L, X, H$	$S(X, Z), U(X, Z)$	Centrifuge test data
Goh & Hefney (2010)	ANN (8-5-1)	$H, AR, P_t, SPT$ @ crown & springline, $w_c, E_s, P_g$	$S_{max}$	148 – MRT tunnel (Singapore)
Kongsomboon et al. (2010)	ANN (14-15-15-1)	$H, D, L, Y$ , geology, WT, $P_t, PR, \theta, P_g, V_g$	$U_{max}$	38 – Chaloe Ratchamongkol MRT & Bangkok water conveyance tunnels (Thailand)
Qiao et al. (2010)	ANN (13-20-1)	$H, L$ , geologies, WT, $P_t, PT, \theta, P_g, V_g$	$S_{max}$	49 – Bangkok MRT tunnel (Thailand)
Tsekouras et al. (2010)	ANN (5-11-3)	Stability, lining placement, $\hat{t}, E_t, Y$	$S_{max}, U_{max}, V_{max}$	7650 – finite difference analyses
Ninic et al. (2011)	ANN (6-14-1)	$P_t, P_g, K, H, X, Y$	$S(X, Y)$	2160 – finite element analyses
Darabi et al. (2012)	ANN (5-17-1)	$c', \phi', E_s, H, D$	$S_{max}$	50 – various projects in Iran & Turkey
Li et al. (2012)	PSO-SVM with chaotic mapping	-	$C_h$	39 – Xiakeng tunnel (China)
Mahdevari & Torabi (2012)	ANN (9-35-28-1); RBF-ANN (9-35-28-1)	$H, GSI, RQD$ , compressive & tensile strength, $c', \phi', E_s, UCS$	$C_{ave}$	60 – Ghomroud water tunnel (Iran)
Mahdevari et al. (2012)	SVM (RBF kernels); ANN (9-35-28-1)	$H, GSI, RQD$ , compressive & tensile strength, $c', \phi', E_s, UCS$	$C_{ave}$	60 – Ghomroud water tunnel (Iran)
Marto et al. (2012)	ANN (9-24-1)	$H, SPT, w_c, c', \phi', E_s, \gamma, v_s, Y$	$S(Y)$	160 – Karaj urban railway tunnel (Iran)
Pourtaghi & Lotfollahi-Yaghin (2012)	Wavelet-ANN (13-10-1)	$H, L$ , geologies, WT, $P_t, PR, P_g, \theta, V_g$	$S_{max}$	49 – Bangkok MRT tunnel (Thailand)
Rafiai & Moosavi (2012)	ANN (11-7-4-2)	R, rock stresses, $c', \phi', E_s, v_s, \psi', \hat{t}, E_t, v_l$	$C_h, C_v$	2500 – finite difference analyses
Adoko et al. (2013)	MARS; ANN (8-20-26-1)	Rock class rating index, $c', \phi', E_s, \gamma, H, Y$ , time	$C_{ave}$	390 - CKTJ-9 high speed railway tunnel (China)
Khatami et al. (2013)	ANN (6-15-1)	Building EI, width, weight. Distance between tunnels, $H, X$	Building settlement	160 – finite element analyses
Mahdevari et al. (2013)	SVM (RBF kernels)	$w_c, \gamma, c', \phi', E_s, k_{sub}$	$C_{ave}$	75 – Amirkabir tunnel (Iran)
Ninic et al. (2013)	PSO-ANN (6-20-1)	$E_s, K, P_t, Y, X, P_g$	$S(X, Y)$	625 – finite element analyses
Ocak & Seker (2013)	ANN (18-9-1); SVM (RBF kernels); GPR (SQ kernels)	18 tunnel, TBM and soil parameters	S	230 – Istanbul metro tunnel (Turkey)
Bouayad & Emeriault (2014)	ANFIS combined with PCA	6 TBM & soil parameters	S	432 – Toulouse subway tunnel (France)

Guo et al. (2014)	Elman-type PSO-RNN (4-20-1)	$H, JF, P_i, V_g$	S	Jiangji subway tunnel (China)
Anghari et al. (2015)	ANFIS; GEP	$H, D, c', \phi', E_s$	$S_{max}$	53 – finite difference analyses
Behnia & Shahriar (2015)	GEP	$H, D, c', \phi', E_s$	$S_{max}$	50 – finite difference analyses
Bouayad et al. (2015)	Partial least squares regression combined with agglomerative hierarchical clustering	11 TBM & tunnel geometry parameters	S	432 – Toulouse subway tunnel (France)
Khamesi et al. (2015)	Fuzzy systems coupled with (a) PSO, (b) ICA and (c) nearest neighbourhood clustering	$K, E_s, s_u$ , soil mass number	S	240 – Karaj subway tunnel (Iran)
Koukoutas & Sofianos (2015)	ANN (14-15-1)	$H, WT$ , geologies, $JF, P_i, PR, T, P_g, V_g$ , excavated material	$S_{max}$	584 – Athens extension (317), Thessaloniki metro tunnels (267; Greece)
Mohammadi et al. (2015)	ANN (6-14-1)	$H$ , soil type, $\gamma, c', \phi', E_s$	$S_{max}$	17 – Niayesh highway tunnel (Iran)
Dindarloo & Siami-Irdemoosa (2015)	CART	$H, D, V_L$ , normalised $V_L, s_u, WT, CM$	$S_{max}$	34 – tunnels from UK, USA, Canada, Thailand, Brazil, Germany
Cao et al. (2016)	RNN combined with Gappy POD	$E_s, P_g$	S	60 – finite element analyses
Hasanipanah et al. (2016)	PSO-ANN (3-4-1)	$K, s_u, E_s$	$S_{max}$	143 – Karaj subway Line 2 tunnel (Iran)
Lai et al. (2016)	ANN (9-?-2)	$H, D, c', \phi', E_s, P_g, V_g, JF, PR$	$S_{max}$ , trough width coefficient	6 – three tunnel projects in China
Wang et al. (2016)	Relevance vector machine (RBF kernels)	$H, Y, P_i, P_g, AR$ , geologies, lagged settlement measurements	S	182 – Wuhan metro Line 2 tunnel (China)
Zhou et al. (2016)	RF (500 trees)	$H, D, c', \phi', E_s, P_g, V_g, JF, PR$	$S_{max}$	26 – Shanghai, Guangzhou and Nanjing tunnels (China)
Bouayad & Emeriault (2017)	ANFIS coupled with PCA and agglomerative hierarchical clustering	6 TBM & soil parameters	S	432 – Toulouse subway tunnel (France)
Kohestani et al. (2017)	RF (270 trees)	$H, L$ , geologies, $P_i, PR, \theta, P_g, V_g$	$S_{max}$	49 – Bangkok MRT tunnel (Thailand)
Naeini & Khalili (2017)	ANFIS	$H, D, c', \phi', E_s$	$S_{max}$	46 – subway tunnels in Iran & Turkey
Zhang et al. (2017)	Wavelet least squares GA-SVM (RBF kernels)	Measured settlement time histories	S	60 – Wuhan metro Line 3 tunnel (China)
Zhou et al. (2017)	RF (500 trees)	Set A: $H, D, V_L$ , normalised $V_L, s_u, WT, CM$ Set B: $H, D, c', \phi', E_s, P_g, V_g, JF, AR$	$S_{max}$ , trough width coefficient	66 – various tunnels worldwide
Fattahi & Babanouri (2018)	Rock engineering systems	$H, L, WT, P_i, PR, \theta, P_g, V_g$ , geologies	$S_{max}$	49 – Bangkok MRT tunnel (Thailand)
Goh et al. (2018)	MARS	$H, AR, P_i, SPTs, wc, E_s, P_g$	$S_{max}$	148 – three MRT tunnels in Singapore
Mehmahad & Zekrabad (2018)	ANN (7-24-1)	$L, H, \gamma, E_s, c', \phi', P_i$	$S_{max}$	181 – Mashhad metro Line 2 tunnel (Iran)
Moeinossadat et al. (2018a)	ANFIS	$H, D, H/D, c', \phi', E_s, P_g, V_g, JF, PR$	$S_{max}$	41 – Shanghai subway Line 2 tunnel (China)
Moeinossadat et al. (2018b)	ANFIS; GEP; Neuro-genetic systems	$H, D, c', \phi', E_s, P_g, V_g, JF, AR$	$S_{max}$	41 – Shanghai subway Line 2 tunnel (China)
Moghaddasi & Noorian-Bidgoli (2018)	ICA-ANN (3-4-1)	$K, s_u, E_s$	$S_{max}$	143 – Karaj subway Line 2 tunnel (Iran)
Sun et al. (2018a)	Multiclass SVM (RBF kernels)	$D, H$ , support stiffness, rock tunnelling quality index	$C_{ave}$	117 – various tunnels worldwide
Chen et al. (2019a)	ANN; RBF-ANN; General regression network	$JF, T, P_i, PR, V_g, H, WT$ , modified SPT, modified DPT, modified UCS	$S_{max}$	200 – Changsha metro Line 4 tunnel (China)

Chen et al. (2019b)	ANN; Wavelet-ANN; General regression ANN; ELM; SVM; RF	JF, $T$ , $P_t$ , PR, $V_g$ , $H$ , WT, modified SPT, modified DPT, modified UCS	$S_{max}$	200 – Changsha metro Line 4 tunnel (China)
Fattahi & Bayatzadehfard (2019)	ANFIS with subtractive clustering; FCM-ANFIS; ANFIS with biogeography-based optimisation	$H$ , $L$ , WT, $P_t$ , PR, $\theta$ , $P_g$ , $V_g$	$S_{max}$	49 – Bangkok MRT tunnel (Thailand)
Hajihassani et al. (2019)	GEP	$H$ , $c'$ , $\phi'$ , $\gamma$ , $v_s$ , $E_s$	$C_{ave}$	118 – Karaj Urban railway Line 2 tunnel (Iran)
Hu et al. (2019)	PSO-ANN; PSO-SVR; PSO-ELM	Measured settlement time histories	S	70 – Zhuhai tunnel (China)
Liu & Liu (2019)	GA-GPR (SE + RQ kernels); GA-SVM (RBF kernels)	$c'$ , $\phi'$ , $v_s$ , $E_s$ , $K$ , $Y$	$C_h$ , $C_v$	Finite difference analyses
Moeinossadat & Anghari (2019)	GEP	$c'$ , $\phi'$ , $\gamma$ , $v_s$ , $E_s$ , $K$ , $H$ , $P_t$ , surface surcharge	$S_{max}$	100 – finite difference analyses
Ramezanshirazi et al. (2019)	ANN (15-30-1)	15 geometric, TBM & soil parameters	$S_{max}$	Milan M5 metro tunnel
Saadallah et al. (2019)	Vector autoregressive with exogenous variables	-	S	160 – finite element analyses
Shi et al. (2019b)	SVM with information granulation using two-layer perceptron kernel	-	$C_{ave}$	Panlongshan tunnel (China)
Zhang et al. (2019a)	RF (91 trees)	JF, $T$ , $P_t$ , PR, $V_g$ , $H$ , WT, modified SPT, modified DPT, modified UCS, ground condition, stoppages	$S_{max}$	294 – Changsha metro Line 4 tunnel set A (China)
Zhang et al. (2019a)	RF (38 - 153 trees)	JF, $T$ , $P_t$ , PR, $V_g$ , $H$ , WT, modified SPT, modified DPT, modified UCS, ground condition	$S_{max}$	265 – Changsha metro Line 4 tunnel set B (China)
Zhang et al. (2019b)	SVM	$H$ , $H/L$ , geologies	$S_{max}$	500 – Huquan-Yangjiawan section of Wuhan metro tunnel (China)
Zhu et al. (2019)	Bayesian networks	Seasonal parameters	S	2762 – Shanghai metro Line 1 (China)
Hajihassani et al. (2020)	PSO-ANN (8-12-1)	$H$ , AR, SPT, $c'$ , $\phi'$ , $\gamma$ , $v_s$ , $E_s$	$S_{max}$ , $i_t$ , $i_l$	123 – Karaj Urban railway Line 2 tunnel (Iran)
Yan et al. (2020)	ANN-SVR-ELM ensemble algorithm	Measured settlement time histories	$S_{max}$	70 – Zhuhai tunnel (China)
Zhang (2020)	MARS	$H$ , AR, $P_t$ , SPTs, $w_c$ , $E_s$ , $P_g$	$S_{max}$	148 – three MRT tunnels in Singapore
Zhang et al. (2020)	ANN-SVR-MARS ensemble algorithm using XGBoost	$H$ , AR, $P_t$ , SPTs, $w_c$ , $E_s$ , $P_g$	$S_{max}$	148 – three MRT tunnels in Singapore

<sup>a</sup>MARS = multivariate adaptive regressive splines; <sup>b</sup> $\kappa$  = slope of soil unload-reload curve, GSI = geological strength index,  $k_{sub}$  = modulus of subgrade reaction; <sup>c</sup> $u$  = horizontal movement,  $i_t$ ,  $i_l$  = transverse and longitudinal inflection point



## FIGURE CAPTION LIST

**Fig. 1** Structure of a single artificial neuron showing mathematical operations performed on the input data

**Fig. 2** Illustration of random forest approach showing structure of individual trees

**Fig. 3** Illustration of  $\epsilon$ -insensitive SVR with slack variables

**Fig. 4** Overview of genetic operators used for genetic algorithm optimisation procedure

**Fig. 5** Overview of imperialist competitive algorithm implementation

**Fig 6** Definition of tunnel geometry, TBM and soil parameters adopted in this study (note pressure balance shield machine shown for illustrative purposes)

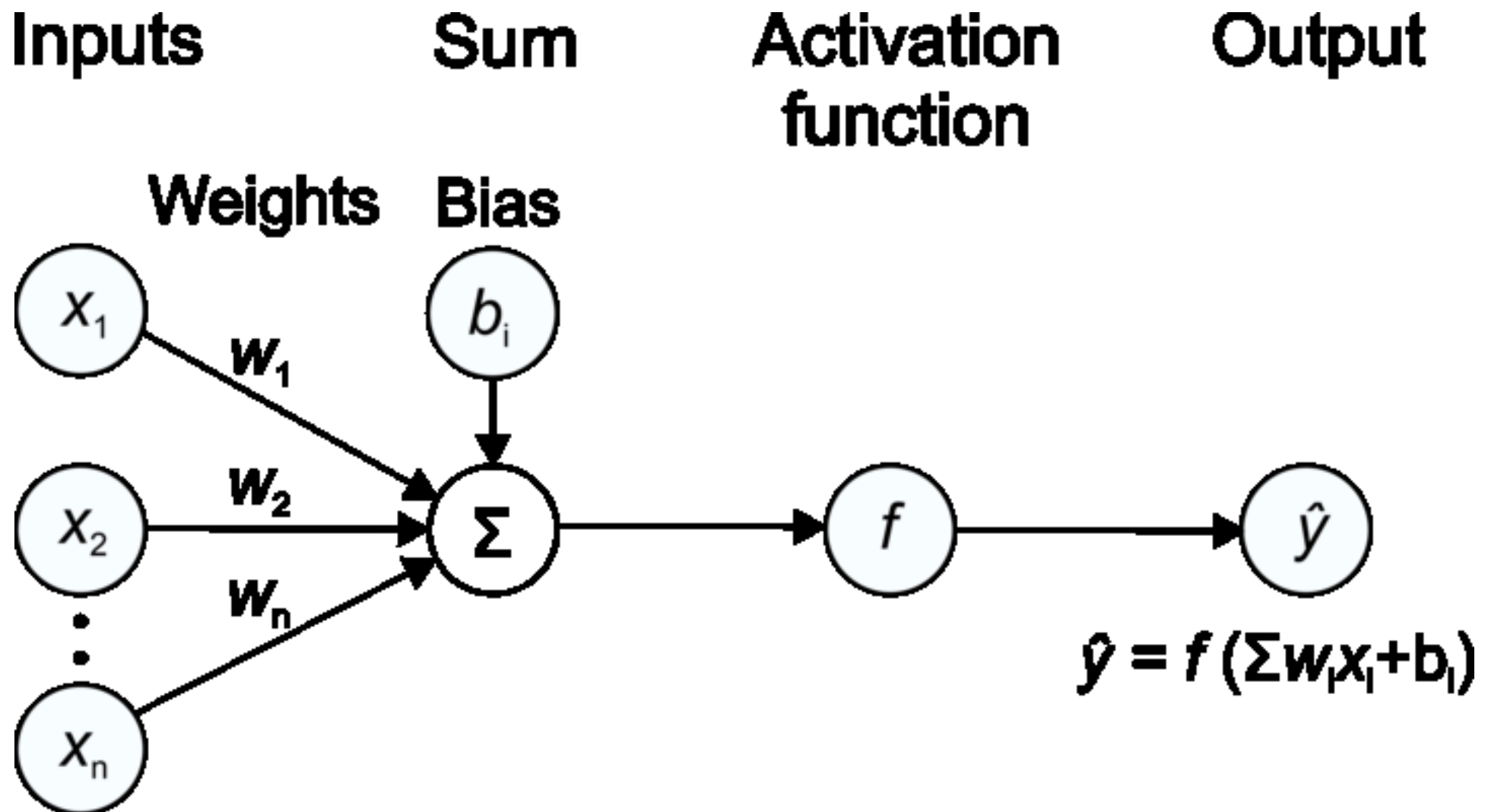
**Fig. 7** Definition of geological identification and forecasting problem

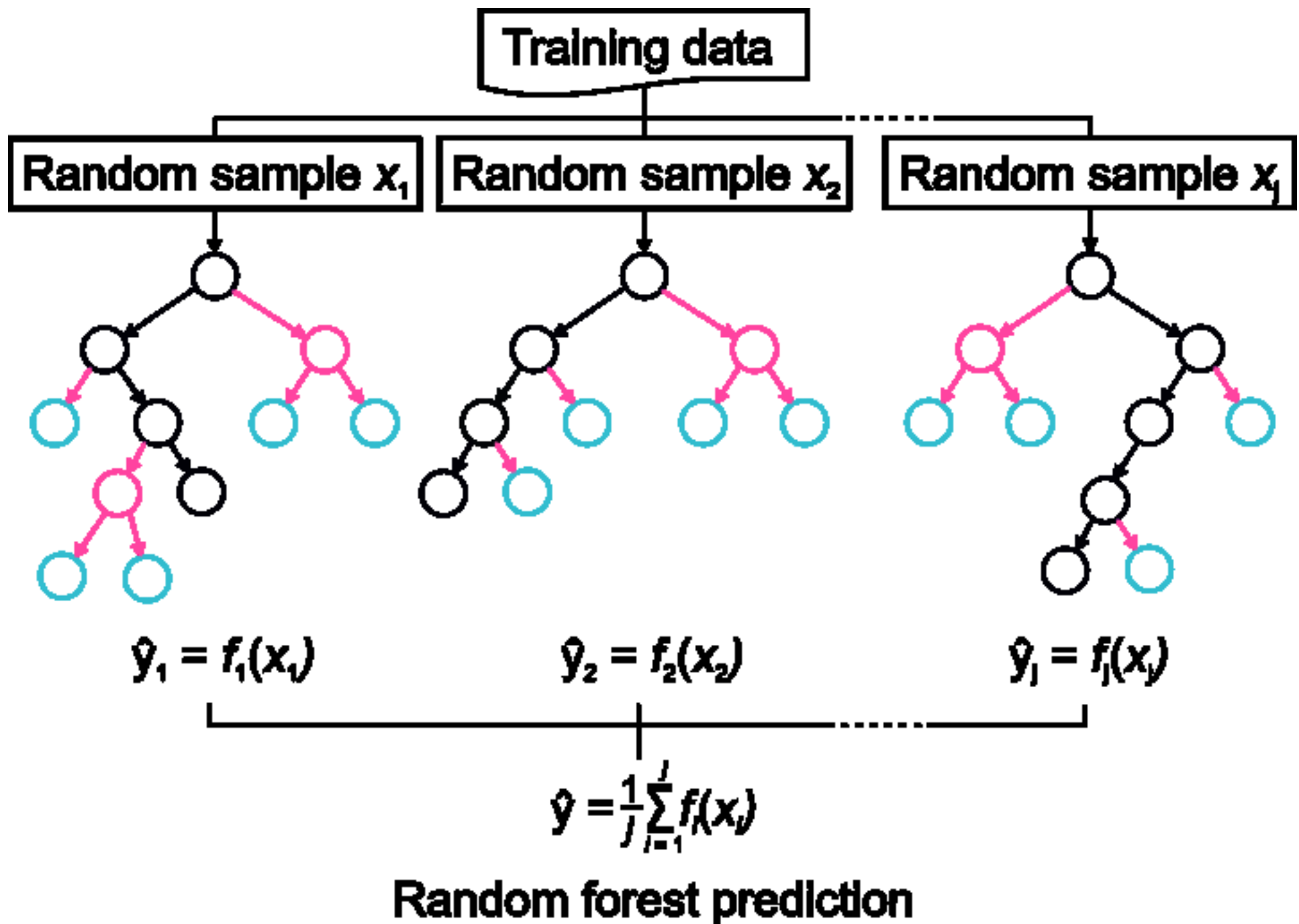
**Fig. 8** Geological interpolation by Kriging documented by Sun et al. (2018)

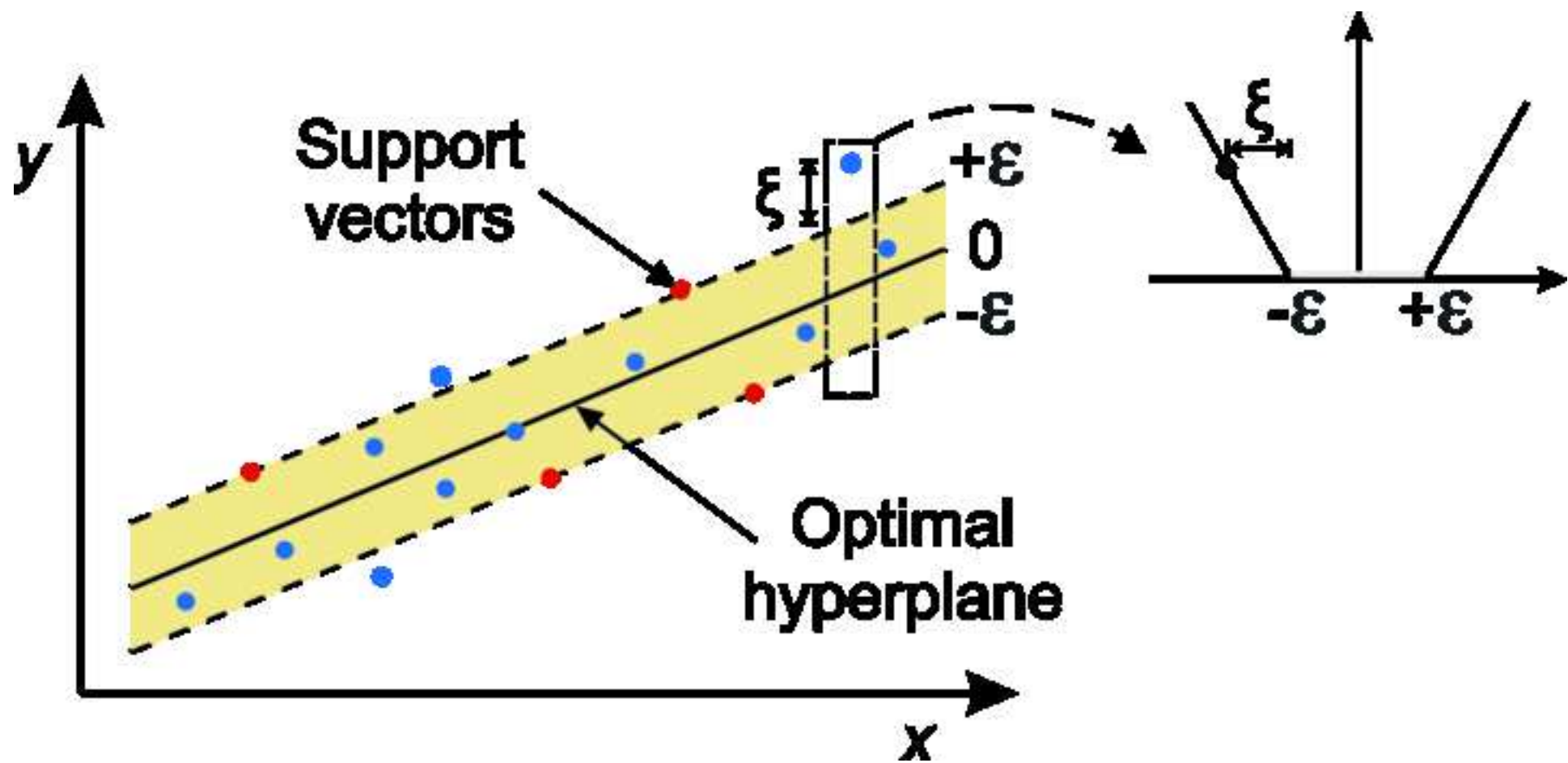
**Fig. 9** Pipeline of the event detection and tracking approach proposed by Wei et al. (2018)

**Fig. 10** Overview of cutterhead design

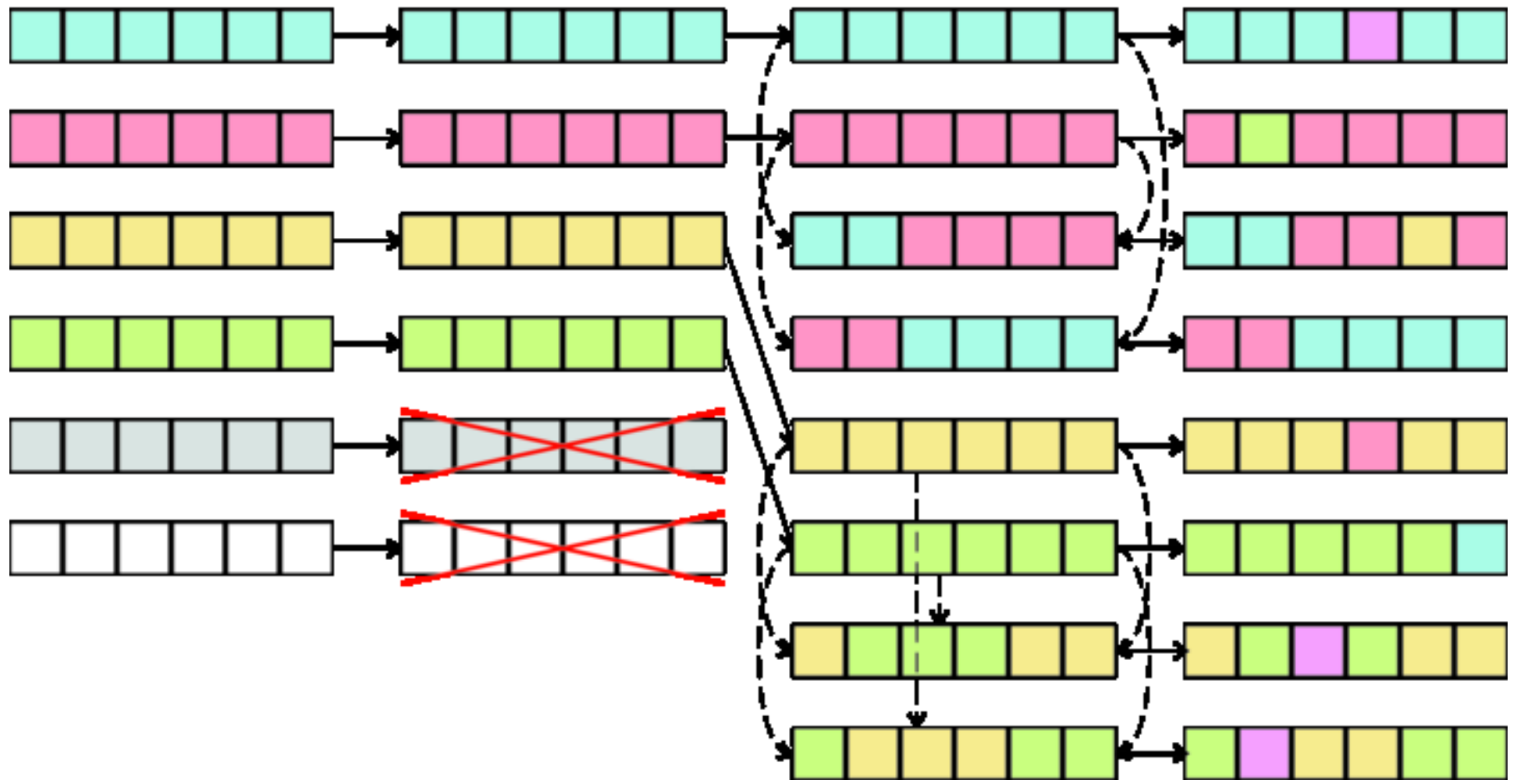
**Fig. 11** Optimal cutterhead layout obtained by Huo et al. (2011): (a) spiral, (b) dynamic star and (c) stochastic

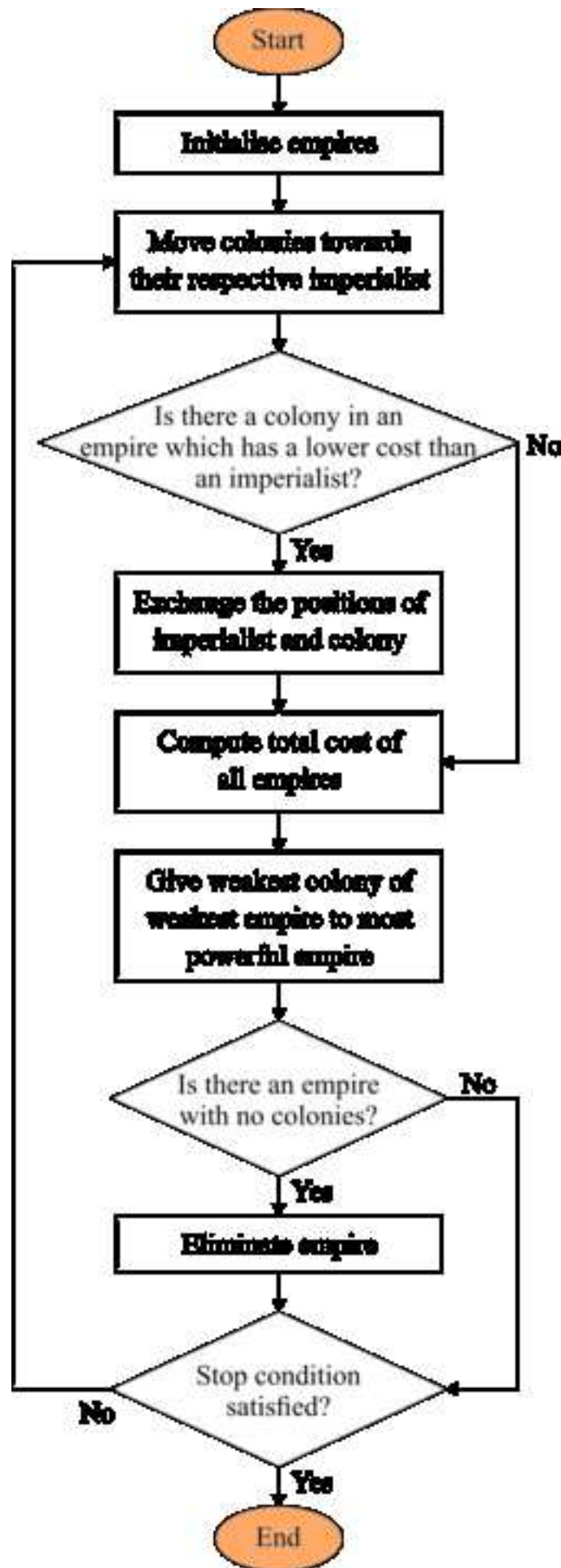


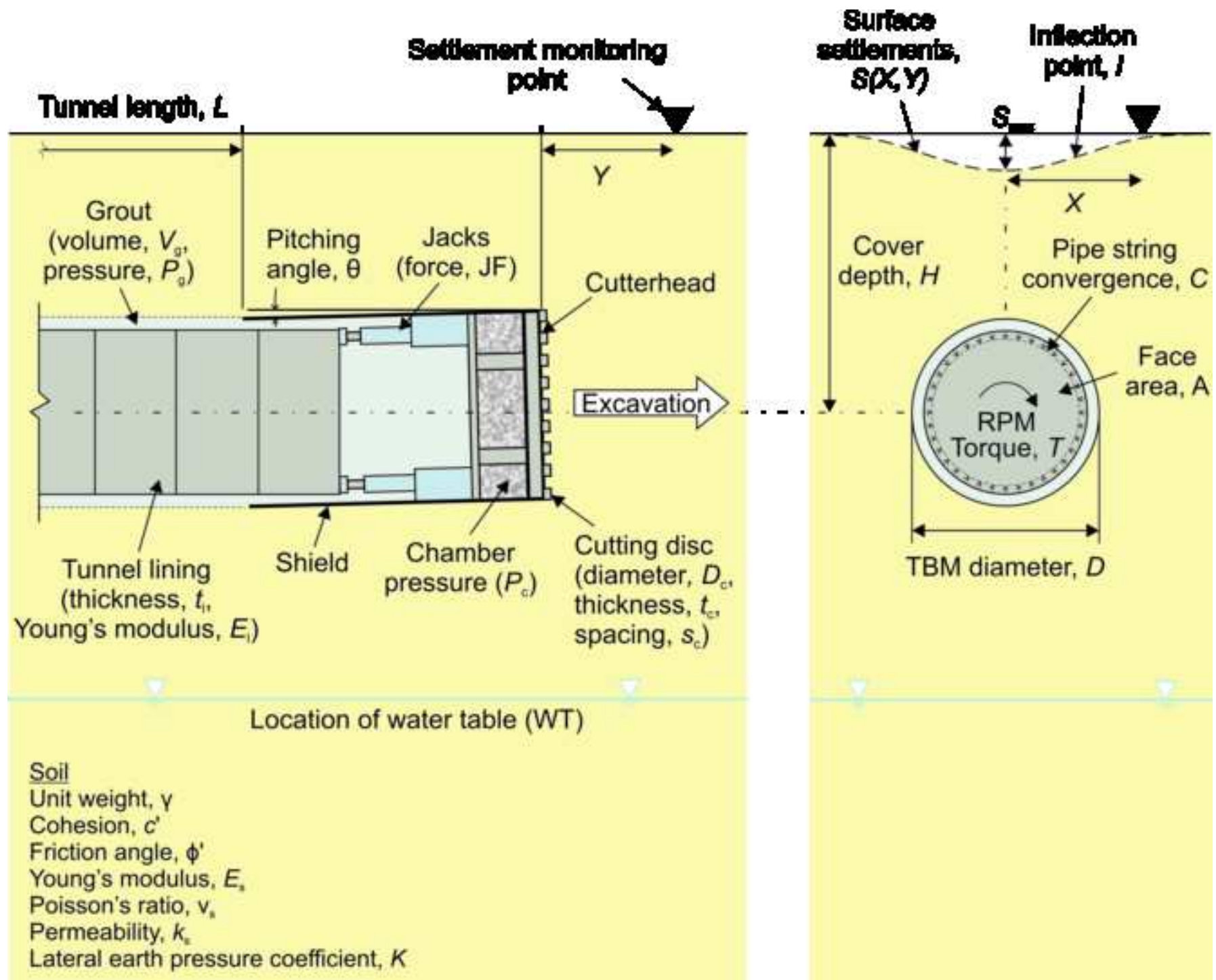


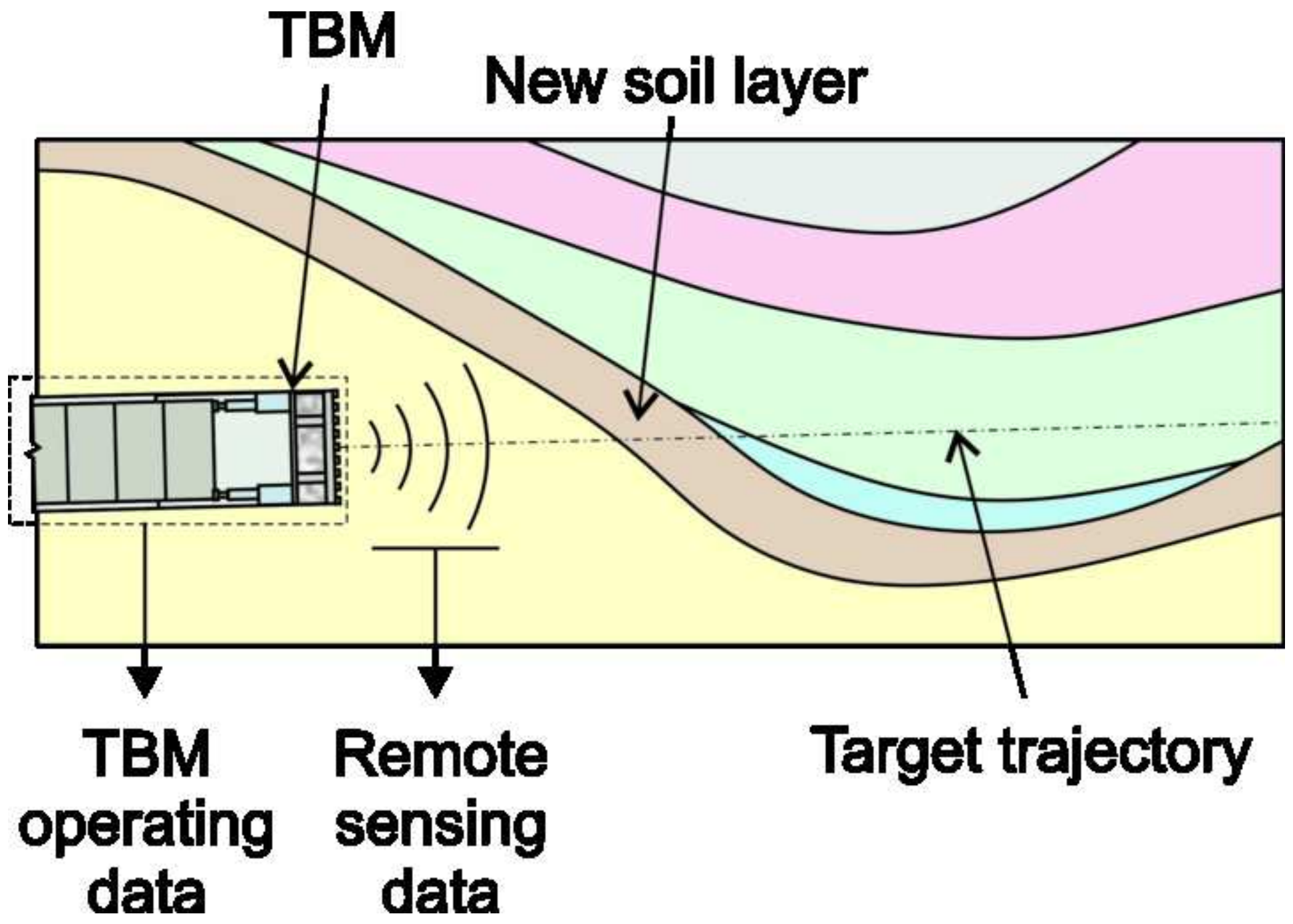


# Evaluation → Selection → Crossover → Mutation



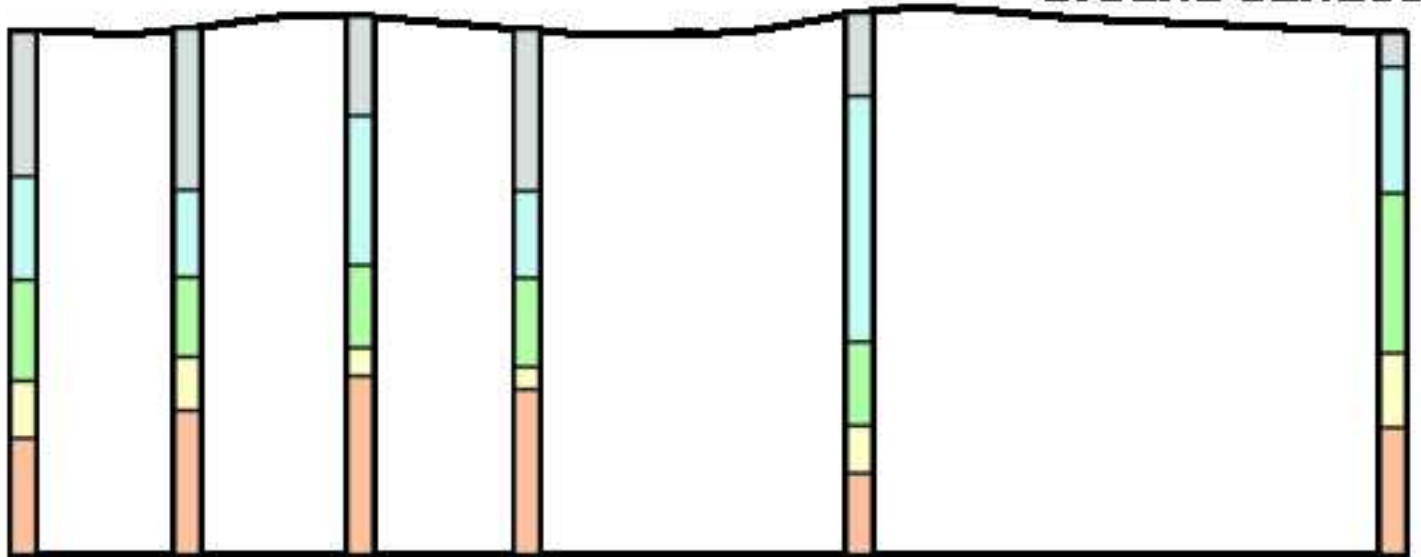






## Discrete borehole data

Ground surface



## Kriging-inferred stratigraphy

Ground surface

